16. Matsuo H, Nakayama A, Sakiyama M, et al. ABCG2 dysfunction causes hyperuricemia due to both renal urate underexcretion and renal urate overload. Sci Rep 2014;4:3755.
17. de Lau LM, Koudstaal PJ, Hofman A, Breteler MM. Serum uric acid levels and the risk of Parkinson disease. Ann Neurol 2005;58:797–800.
18. Schwarzschild MA, Schwid SR, Marek K, et al. Serum urate as a predictor of clinical and radiographic progression in Parkinson disease. Arch Neurol 2008;65:716–723.
19. Gonzalez-Aramburu I, Sanchez-Juan P, Jesus S, et al. Genetic variability related to serum uric acid concentration and risk of Parkinson's disease. Mov Disord 2013;28:1737–1740.
20. Facheris MF, Hicks AA, Minelli C, et al. Variation in the uric acid transporter gene SLC2A9 and its association with AAO of Parkinson's disease. J Mol Neurosci 2011;43:246–250.
21. Uchida Y, Ohtsuki S, Katsukura Y, et al. Quantitative targeted absolute proteomics of human blood-brain barrier transporters and receptors. J Neurochem 2011;117:333–345.
22. Schwarzschild MA, Ascherio A, Beal MF, et al. Inosine to increase serum and cerebrospinal fluid urate in Parkinson disease: a randomized clinical trial. JAMA Neurol 2014;71:141–150.

SCIENTIFIC REPORTS

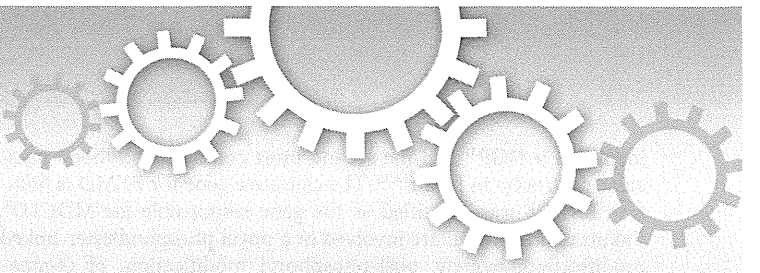

OPEN

SUBJECT AREAS:
DISEASES
GENETICS

Received
8 October 2014

Accepted
13 January 2015

Published
9 February 2015

Correspondence and requests for materials should be addressed to T.T. (toda@med.kobe-u.ac.jp)

Fukutin is prerequisite to ameliorate muscular dystrophic phenotype by myofiber-selective LARGE expression

Yoshihisa Ohtsuka[1], Motoi Kanagawa[1], Chih-Chieh Yu[1], Chiyomi Ito[1], Tomoko Chiyo[2], Kazuhiro Kobayashi[1], Takashi Okada[2], Shin'ichi Takeda[2] & Tatsushi Toda[1]

[1]Division of Neurology/Molecular Brain Science, Kobe University Graduate School of Medicine, Kobe, 650-0017, Japan, [2]Department of Molecular Therapy, National Institute of Neuroscience, National Center of Neurology and Psychiatry, Kodaira, 187-8502, Japan.

α-Dystroglycanopathy (α-DGP) is a group of muscular dystrophy characterized by abnormal glycosylation of α-dystroglycan (α-DG), including Fukuyama congenital muscular dystrophy (FCMD), muscle-eye-brain disease, Walker-Warburg syndrome, and congenital muscular dystrophy type 1D (MDC1D), etc. LARGE, the causative gene for MDC1D, encodes a glycosyltransferase to form [-3Xyl-α1,3GlcAβ1-] polymer in the terminal end of the post-phosphoryl moiety, which is essential for α-DG function. It has been proposed that LARGE possesses the great potential to rescue glycosylation defects in α-DGPs regardless of causative genes. However, the in vivo therapeutic benefit of using LARGE activity is controversial. To explore the conditions needed for successful LARGE gene therapy, here we used *Large*-deficient and *fukutin*-deficient mouse models for MDC1D and FCMD, respectively. Myofibre-selective LARGE expression via systemic adeno-associated viral gene transfer ameliorated dystrophic pathology of *Large*-deficient mice even when intervention occurred after disease manifestation. However, the same strategy failed to ameliorate the dystrophic phenotype of *fukutin*-conditional knockout mice. Furthermore, forced expression of *Large* in *fukutin*-deficient embryonic stem cells also failed to recover α-DG glycosylation, however coexpression with *fukutin* strongly enhanced α-DG glycosylation. Together, our data demonstrated that fukutin is required for LARGE-dependent rescue of α-DG glycosylation, and thus suggesting new directions for LARGE-utilizing therapy targeted to myofibres.

α-Dystroglycanopathy (α-DGP) is a genetically and clinically heterogeneous group of muscular dystrophy[1,2] for which more than 15 causative genes have been identified[3–21]: *POMT1, POMT2, POMGnT1, fukutin, FKRP, LARGE, ISPD, GTDC2* (*POMGnT2*), *DAG1, TMEM5, B3GALNT2, SGK196* (*POMK*), *B3GNT1* (*B4GAT1*), *GMPPB, DOLK, DPM1, DPM2 and DPM3*. Regardless of the causative gene, α-DGP is characterized by abnormal glycosylation of α-DG, indicating that the disease is associated with defects in the glycosylation pathway for α-DG. α-DG is a cell surface receptor for matrix and synaptic proteins such as laminins, agrin, perlecan, neurexin, and pikachurin[22,23]. A unique *O*-mannosyl glycosylation is required for the ligand-binding activity of α-DG, and abnormal glycosylation leads to reduced ligand-binding activity[24,25]. α-DG also interacts with a transmembrane β-DG, which in turn binds to intracellular dystrophin[23]. Thus, proper glycosylation of α-DG is necessary for the connection between the basement membrane and cytoskeleton. Disruption of this linkage is thought to cause myofibre membrane weakness, leading to disease-predisposing muscle cell necrosis[26]. Although myofibres can regenerate after necrosis, it has been shown that muscle regeneration activity is impaired in α-DGP[27]. Thus, α-DG glycosylation is important for maintenance of skeletal muscle viability and defects in this process underlie the pathogenesis of α-DGP.

α-DGP includes Fukuyama congenital muscular dystrophy (FCMD), muscle-eye-brain disease (MEB), Walker-Warburg syndrome (WWS), and several types of congenital muscular dystrophies (MDCs) and limb-girdle muscular dystrophies (LGMDs)[1,2]. The clinical spectrum of α-DGP is wide; the most severe cases exhibit congenital muscular dystrophy with structural abnormalities in the brain and eyes, whereas the mildest form presents as adult-onset LGMD with no central nervous system involvement[28–30]. In addition, there is no clear genotype-phenotype correlation. Thus, it has been proposed that α-DGPs can be classified into three broad phenotypic groups, MDDG (muscular dystrophy dystroglycanopathy) type A, B and C[29]: MDC with brain/eye abnormalities (A), MDC with milder brain structural abnormalities (B), and LGMD (C). FCMD is the first

identified α-DGP[31] and the second most common childhood muscular dystrophy in Japan[32,33]. The causative gene for FCMD is *fukutin*[6]. *LARGE* was identified as the gene responsible for MDC1D[8]. Fukutin and LARGE are involved in a novel phosphodiester-linked modification, namely, post-phosphoryl modification, of *O*-mannnose on α-DG[24,34]. Although the exact function of fukutin is unknown, LARGE was recently shown to be a glycosyltransferase that catalyses the formation of a repeating [-3Xyl-α1,3GlcAβ1-] polymer, which is modified on the distal end of the post-phosphoryl moiety[35]. These repeating units likely serve as the ligand-binding domain of α-DG[36]. Interestingly, overexpression of LARGE causes hyperglycosylation of α-DG with increased ligand-binding activity not only in wild-type and *Large*-deficient muscle cells, but also in cells from WWS, MEB, FCMD patients and mouse models[37]. This finding inspired a novel therapeutic strategy based on the unique activity of LARGE—modulation of LARGE activity can be a versatile treatment for α-DGP, regardless of the causative gene.

After this breakthrough finding, several reports showed that overexpression of LARGE in mice induced hyperglycosylation of α-DG in skeletal muscle of α-DGP mouse models such as *POMGnT1*- and *FKRP*-deficient[38,39]. However, LARGE overexpression in cells lacking GTDC2 expression or POMT1 activity did not induce hyperglycosylation of α-DG[9,40]. Moreover, some studies have shown the beneficial effects of LARGE overexpression in *POMGnT1*- or *FKRP*-mutant mice[38,39], but others showed a deterioration in *FKRP*- or *fukutin*-mutant mice crossed with LARGE-overexpressing transgenic mice[41,42]. Thus, it remains unclear whether LARGE could be a target molecule for α-DGP treatment. We hypothesized that the conditions for LARGE expression such as way of gene delivery, timing of intervention, and target cells may affect α-DG glycosylation and therapeutic consequences. Here, we examined therapeutic benefits of myofibre-selective *Large* gene expression after disease manifestation in *Large*- or *fukutin*-deficient α-DGP mouse models. Our data also showed that fukutin is a prerequisite for LARGE-dependent rescue of α-DG glycosylation.

Results

Myofibre-selective expression of *Large* after disease onset restores α-DG glycosylation and ameliorates dystrophic pathology of *Large^{myd}* mice. We performed systemic *Large* gene delivery after disease manifestation and myofibre-selective *Large* gene expression in α-DGP mouse models. For this purpose, we constructed recombinant adeno-associated virus (AAV) 9 vectors containing the *Large* cDNA under the myofibre-selective muscle creatine kinase (MCK) promoter (AAV9-MCK-*Large*). We first examined the therapeutic benefits of muscle-selective LARGE expression in *Large*-deficient *Large^{myd}* mice. New-born *Large^{myd}* mice (1 week old) showed no signs of muscle pathology (Fig. 1a), but at 4 weeks of age, the *Large^{myd}* skeletal muscles showed signs of muscular dystrophy such as necrotic and regenerating fibres (Fig. 1a). After 4 months, *Large^{myd}* mice showed severe dystrophic pathology in the hind-limb muscles (Fig. 1a). The dystrophic changes include the presence of myofibres with loss of polygonal contour, high population of regenerating fibres with centrally located nuclei, and infiltrations of macrophages and connective tissues. Therefore, we administered intravenous AAV9-MCK-*Large* via the tail vein to 5-week-old *Large^{myd}* mice exhibiting dystrophic symptoms, and then analysed α-DG glycosylation status and therapeutic effects after 5 months. Glycosylation status was evaluated by assessing the reactivity of the monoclonal IIH6 antibody, which recognizes properly glycosylated α-DG[25].

Western blot analysis confirmed LARGE was overexpressed in AAV-treated *Large^{myd}* mice; consequently, the reactivity of IIH6 antibody exceeded even the baseline levels observed in untreated heterozygous animals (Fig. 1b). Immunofluorescence analysis also confirmed increased IIH6-reactivity in the treated *Large^{myd}* skeletal muscles (Fig. 1c). Haematoxylin and eosin (H&E) staining of skeletal muscles indicated decreases in the number of necrotic fibres and recovery of the polygonal contour of myofibres in AAV-treated *Large^{myd}* versus untreated *Large^{myd}* mice (Fig. 1d). The number of muscle fibres with centrally located nuclei as well as infiltration of connective tissues and macrophages were significantly reduced in comparison to the findings obtained for untreated *Large^{myd}* mice (Fig. 2a–c). After the AAV-injection, we tracked changes in grip strength, body weight, and serum creatine kinase (CK). Our results showed significant improvements of these parameters even 4 weeks after the injection (Fig. 2d–f). These results demonstrated that myofibre-selective LARGE expression in *Large^{myd}* mice via systemic administration ameliorates the dystrophic pathology even if the initial intervention occurs after onset.

***Large* gene therapy failed to restore glycosylation and ameliorate muscle pathology of *fukutin*-deficient α-DGP models.** LARGE overexpression increases glycosylation and ligand-binding activity of α-DG in *fukutin*-deficient cells from FCMD patients[37]. We examined whether the muscular dystrophic phenotype of *fukutin*-deficient mice can be improved by LARGE overexpression in vivo. We used muscle precursor cell (MPC)-selective *fukutin*-deficient conditional knock-out (cKO) mice as a *fukutin*-deficient model (Myf5-*fukutin*-cKO mice)[27]. Myf5-*fukutin*-cKO mice showed loss of IIH6-positive glycosylation of α-DG in the skeletal muscles at birth[27]. The dystrophic pathology begins around 4 weeks of age and becomes severe at 12 weeks[27]. We administered intravenous AAV9-MCK-*Large* into 4-week-old Myf5-*fukutin*-cKO mice via the tail vein, and then analysed the glycosylation status of α-DG and therapeutic efficacy after 2 months. Interestingly, although we observed expression of LARGE protein in the AAV-treated Myf5-*fukutin*-cKO skeletal muscles, IIH6-positive α-DG was hardly produced in AAV-treated Myf5-*fukutin* cKO mice (Fig. 3a). Immunofluorescence staining also confirmed failure to restore IIH6-positive glycosylation of α-DG by AAV-treatment in Myf5-*fukutin*-cKO mice (Fig. 3b). H&E staining of skeletal muscles and quantitative muscle pathology showed no significant improvement with AAV treatment (Fig. 3c and Fig. S1a–c). In addition, we found no evidence to support improvements in grip strength, body weight, and serum CK activity after AAV treatment (Fig. S1d–f). These data indicate that the failure to restore α-DG glycosylation in Myf5-*fukutin*-cKO mice is associated with failure of LARGE therapeutic efficacy.

The amount of LARGE protein expressed in the AAV-treated Myf5-*fukutin*-cKO mice was comparable to that in AAV-treated *Large^{myd}* (Fig. 3a). α-DG glycosylation was recovered in *Large^{myd}* skeletal muscle after AAV9-MCK-*Large* treatment, suggesting something other than protein expression levels is responsible for the failure of glycosylation recovery in Myf5-*fukutin*-cKO mice. We hypothesized that complete loss of fukutin caused failure to build the part of post-phosphoryl moiety, which may be required for LARGE-dependent glycosylation; therefore, even excess LARGE protein could not form the [-3Xyl-α1,3GlcAβ1-] polymer on α-DG. To test this hypothesis, we expressed LARGE in *fukutin*-null embryonic stem (ES) cells. Transfection of the *fukutin* cDNA restored IIH6 reactivity in *fukutin*-null ES cells, but transfection of the *Large* cDNA failed to restore α-DG glycosylation, although LARGE expression in wild-type ES cells produced strong IIH6-reactivity (Fig. 4). When the *fukutin* and *Large* cDNAs were co-transfected into *fukutin*-null ES cells, we observed increases in IIH6-reactivity in comparison to *fukutin* singly transfected cells although expression levels of both fukutin and LARGE were much lower than they were in each single transfection (Fig. 4, lanes 6–8). These data show that fukutin-dependent modification is a prerequisite for LARGE-dependent formation of [-3Xyl-α1,3GlcAβ1-] repeating units.

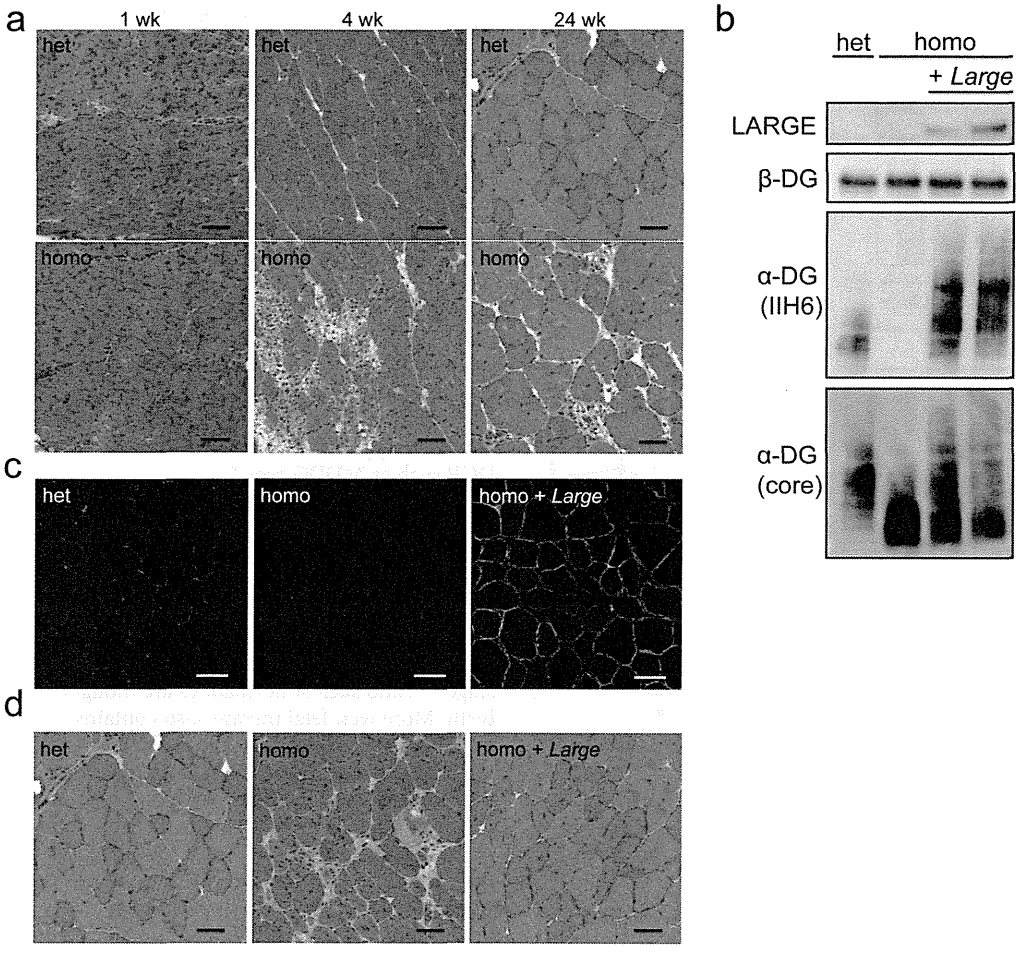

Figure 1 | Systemic gene transfer of *Large* into *Large*^{myd} mice after onset. (a) Histopathological analysis (H&E staining) of the skeletal muscle of *Large*^{myd} (homo) and heterozygous (het) mice at 1, 4, and 24 weeks of age. Bar = 50 μm. (b–d) AAV9-MCK-*Large* was administered to 5-week-old *Large*^{myd} mice via the tail vein; after 5 months, the skeletal muscles were harvested and analysed for α-DG glycosylation (b, c) and histology (d). LARGE was detected by western blotting of total lysates (b). β-DG was used as a loading control. DG proteins enriched with WGA-beads were analysed by western blotting to assess α-DG glycosylation (b). The full-length blots with α-DG (IIH6), α-DG (core), LARGE, and β-DG are presented in Supplementary Figure S2a–d, respectively. Immunofluorescence analysis with IIH6 antibody confirmed the increase in α-DG glycosylation (c). H&E staining of the tibialis anterior muscle indicated amelioration of the muscular dystrophic phenotype after treatment with AAV9-MCK-*Large* (d). Het, *Large*^{myd} heterozygous controls; homo, untreated *Large*^{myd} homozygous mice; and homo + *Large*, *Large*^{myd} homozygous mice with AAV9-MCK-*Large* treatment. Bar = 50 μm.

Discussion

It has been widely recognized that LARGE possesses the great potential to rescue glycosylation defects of α-DG regardless of causative genes for α-DGP, however, therapeutic benefits of using LARGE activity is controversial. To assess the feasibility of LARGE-utilizing therapy, in this study we explored the conditions needed for successful *Large* gene therapy. We demonstrated for the first time that AAV-mediated *Large* gene expression targeted to myofibres is therapeutically beneficial in a *Large*-deficient α-DGP model even when the intervention is performed after disease manifestation. On the other hand, the same strategy failed to restore α-DG glycosylation in *fukutin*-deficient skeletal muscles and ES cells, suggesting that fukutin is required for LARGE-utilizing therapeutic strategy.

Several reports have shown that AAV-mediated LARGE expression, which was driven by the chicken β-actin (CB) promoter, restored glycosylation of α-DG in *Large*^{myd} mice[38,39]. However, expression of exogenous genes by non-selective promoter such as the CB promoter in various non-muscle cells may be detrimental. For example, because glycosylation levels of α-DG and the expression levels of LARGE change during muscle differentiation and regeneration[36], excess glycosylation may disturb cellular homeostasis and tissue regeneration. In fact, LARGE overexpression in C2C12 myoblasts impairs differentiation[42]. Furthermore, there may be situations or cells in which glycosylation is physiologically unnecessary even in wild-type tissues[34]. Although AAV-mediated *Large* gene transfer using the CB promoter rescued the muscular dystrophic phenotype in *Large*^{myd} mice[38,39], this study was designed to introduce viral vectors into new-born pups; thus, it is likely that α-DG restores proper glycosylation before disease manifestation, preventing disease-causing myofibre necrosis. However, in humans, clinical and genetic diagnoses of α-DGP are made after disease manifestation, making gene delivery in new-borns unfeasible. We demonstrated that myofibre-selective expression of LARGE ameliorated the dystrophic phenotype of *Large*^{myd} mice, and the intervention even after disease manifestation was effective by using systemic AAV-mediated gene delivery. The effect continues at least for 5 months after the intervention, the longest period observed in gene therapy studies of α-DGP mouse models. Myofibre-selective rescues of fukutin or LARGE expression by AAV gene transfer or crossing with transgenic mice improved the dystrophic phenotypes of Myf5-*fukutin*-cKO or

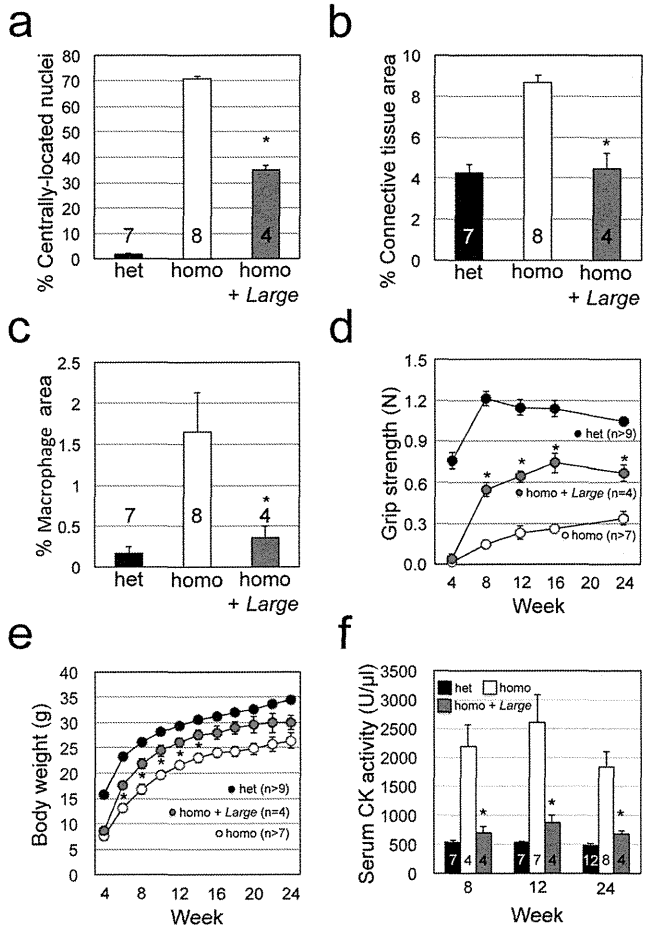

Figure 2 | Quantitative analysis of the therapeutic effects of AAV9-MCK-*Large* treatment in *Large*^{myd} mice. Amelioration of dystrophic histology after AAV9-MCK-*Large* treatment was evaluated by quantifying muscle fibres with centrally located nuclei (a; $P = 0.007$), measuring infiltration of connective tissue by collagen I-immunofluorescence staining (b; $P = 0.007$) and infiltration of macrophages by F4/80-immunofluorescence staining (c; $P = 0.011$). Therapeutic efficacy over time was evaluated by grip strength (d; $P = 0.007$, 0.006, 0.008, and 0.014 for 8, 12, 16, and 24 weeks), body weight (e; $P = 0.019$, 0.019, 0.024, 0.017, and 0.032 for 6, 8, 10, 12, and 14 weeks), and serum CK activity (f; $P = 0.021$, 0.008, and 0.011 for 8, 12, and 24 weeks). Data shown are mean ± s.e.m. for each group (*n* is indicated in the graph). $*P \leq 0.05$ vs. non-treated *Large*^{myd} homozygous mice (Mann–Whitney U test). Het, *Large*^{myd} heterozygous controls; homo, untreated *Large*^{myd} homozygous mice; and homo + *Large*, *Large*^{myd} homozygous mice with AAV9-MCK-*Large* treatment.

Large^{myd} mice[27,43], supporting the validity of myofibre-selective gene rescue for treatment of α-DGP. We propose that myofibre-targeting rescue/reinforcement of glycosylation is an effective treatment for α-DGP.

We also examined the potential of LARGE as a therapeutic target for *fukutin*-deficient α-DGP; however, our data showed that LARGE expression failed to restore α-DG glycosylation in *fukutin*-null myofibres and ES cells. LARGE synthesises [-3Xyl-α1,3GlcAβ1-] repeating units in the terminal end of the post-phosphoryl moiety, which is modified on phospho-mannose in the Core M3 structure, GalNAc-GlcNAc-Man(P)-O[24,35,44]. The activities of POMT and GTDC2 are required for Core M3 synthesis and fukutin mediates formation of the post-phosphoryl modification[24,34,44]. In cells lacking POMT activity or GTDC2 expression, LARGE overexpression failed to induce hyperglycosylation or restore glycosylation of α-DG[9,40]. Thus, even when overexpressed, LARGE requires the Core M3 structure and fukutin-dependent modification in order to form the [-3Xyl-α1,3GlcAβ1-] repeating units. However, several reports have shown LARGE-dependent glycosylation recovery in genetically distinct α-DGP models[38,39], which seems contradictory but can be explained by the presence of residual glycosylation of α-DG. Presumably, α-DG is hypoglycosylated in such cells, but there might be a small amount of normally glycosylated α-DG species produced by residual activity of the mutant gene products. In fact, the *fukutin*-knock-in and *POMGnT1*-KO mice showed slight reactivity against IIH6 antibody, indicating the presence of normally glycosylated α-DG[45,46]. In such cases, LARGE can reinforce [-3Xyl-α1,3GlcAβ1-] repeats on the small amount of residual Core M3 structure. Importantly, many mild cases of FCMD patients show the presence of a small fraction of normally glycosylated α-DG[30]. Thus, the concept of LARGE modulation therapy remains attractive for a wide range of mild cases of α-DGP such as MDDG type C.

An important issue when considering therapeutic applications is that α-DGP is accompanied by central nervous system abnormalities including severe defects in structural development and mental retardation[28,29]. Although the AAV9 vector delivers genes to central nervous tissues[47], there are many obstacles to treatment for developing central nervous tissues. For example, the structural abnormalities in the central nervous system occur during fetal developing stage[48,49], and such abnormalities are thought to be irreversible after birth. Moreover, fetal therapy also contains many concerns such as ethical, legal, technical, and clinical safety issues. However, improvement of muscle functions via muscle-targeting strategies will improve patients' activities of daily living and caregivers' burdens, and may have an impact on patient mental development. We propose that gene therapy is an effective approach to α-DGP even after disease progression, and that LARGE therapy may be applied to mild cases of α-DGP. Our study will provide a new direction for therapeutic approached to α-DGP.

Methods

Animals. *Large*-deficient *Large*^{myd} mice were from Jackson Laboratories. Generation of muscle precursor cell (MPC)-selective *fukutin* conditional knock-out (cKO) mice (Myf5-*fukutin*-cKO mice) was described previously[27]. All animal procedures were approved by the Animal Care and Use Committee of Kobe University Graduate School of Medicine (P120202-R2) in accordance with the guidelines of the Ministry of Education, Culture, Sports, Science and Technology (MEXT) and the Japan Society for the Promotion of Science (JSPS). The animals were housed in cages (2–4 mice per cage) with wood-chip bedding in an environmentally controlled room (25°C, 12 h light-dark cycle) and provided food and water *ad libitum* at the animal facility of Kobe University Graduate School of Medicine. Well-trained and skilled researchers and experimental technicians, who have knowledge of methods to prevent unnecessary and excessive pain, handled the animals and performed the experiments. Euthanisation was done by cervical dislocation. At sacrifice, the muscles were harvested and snap-frozen in liquid nitrogen (for biochemistry) or in liquid-nitrogen-cooled isopentane (for immunofluorescence and histology). The number and ages of the animals used in each experiment are indicated in the Figure legends and graphs.

Adeno-associated viral gene transfer and evaluation of therapeutic efficacy. To generate a *Large*-encoding AAV9 vector, the complete open reading frame of the mouse *Large* gene was cloned into pAAV-IRES-hrGFP[50]. The MCK promoter was subcloned from AAV-MCKLacZ[51]. The recombinant *Large*-encoding AAV9 vector (AAV9-MCK-*Large*) was produced as described[50]. The AAV9-MCK-*Large* viral vectors (5×10^{11} vector genome) were injected into *Large*^{myd} (n = 4) and Myf5-*fukutin* cKO (n = 6) mice via tail vein at 4–5 weeks of age. Before the injection, body weight, grip strength, and serum CK activity were measured. These clinical parameters (body weight, grip strength, and serum CK activity) were continuously measured until the AAV-treated mice were sacrificed for histological evaluation (the time points of the clinical tests were shown in the figures). The H&E and immunofluorescence images shown in the figures are representative of the AAV-treated and non-treated mice.

Quantitative evaluation of muscle pathology was performed by assessing the number of myofibres with centrally located nuclei at least 1,000 fibres. Macrophage and connective tissue infiltration was quantified by analysing the immunofluorescence signals of F4/80-positive and collagen I-positive areas with Image J software. Serum CK activity was measured with the CPK kit (WAKO). Grip strength was measured for 10 consecutive trials for each mouse using a strength meter (Ohara Ika

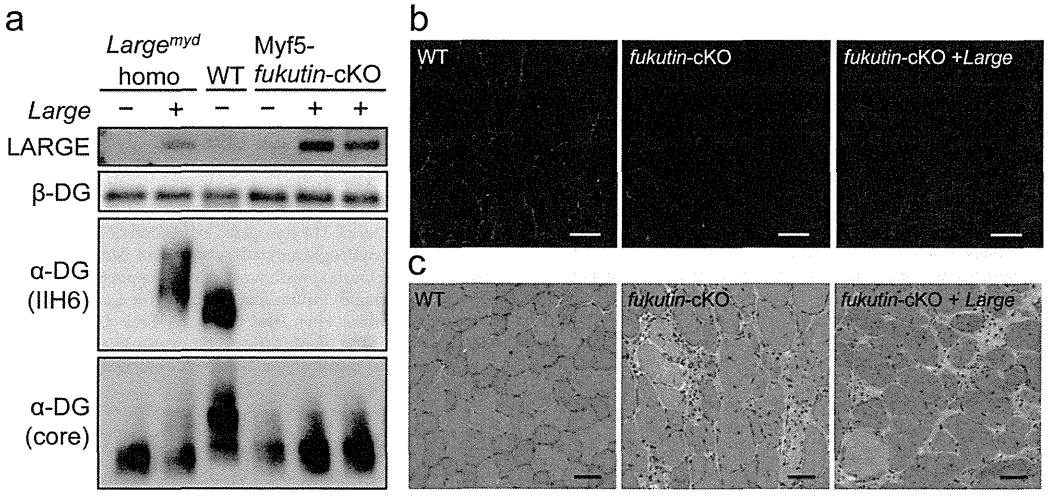

Figure 3 | Systemic gene transfer of *Large* into Myf5-*fukutin* cKO mice after onset. AAV9-MCK-*Large* was administered to 4-week-old Myf5-*fukutin* cKO mice via tail vein injection; after 2 months, the skeletal muscles were harvested and analysed for α-DG glycosylation (a, b) and histology (c). Although LARGE was expressed (a), the levels of α-DG glycosylation were unchanged in AAV-treated Myf5-*fukutin*-cKO mice (a, b). H&E staining for the tibialis anterior muscle did not show improvement of the muscular dystrophic phenotype of Myf5-*fukutin*-cKO mice (c). WT, litter control mice (*fukutin*$^{lox/lox}$ without cre-transgene); *fukutin*-cKO, untreated Myf5-*fukutin*-cKO mice; and *fukutin* cKO + *Large*, Myf5-*fukutin*-cKO mice with AAV9-MCK-*Large* treatment. Bar = 50 μm. The full-length blots with α-DG (IIH6), α-DG (core), LARGE, and β-DG are presented in Supplementary Figure S2e-h, respectively.

Sangyo Co. Ltd., Tokyo); 20% of the top and bottom values were excluded to obtain the mean. Statistical analysis was performed to determine means and s.e.m.; *P*-values <0.05 were considered significant (Mann–Whitney U test).

Antibodies. Antibodies for western blotting and immunofluorescence were as follows: mouse monoclonal antibody 8D5 against β-DG (Novocastra); mouse monoclonal antibody IIH6 against α-DG (Millipore); rat monoclonal antibody against mouse F4/80 (BioLegend); rabbit polyclonal antibody against collagen I (AbD Serotec); mouse monoclonal antibody against FLAG tag (Sigma); and rabbit polyclonal antibody against c-Myc tag (Santa Cruz). Rabbit polyclonal antibody against LARGE was raised using recombinant human LARGE protein expressed in *E. coli*. Antisera were purified by Melon gel IgG purification kit (Pierce). Rat monoclonal antibody against the α-DG core protein (3D7) was generated from a α-DG-Fc fusion protein[52].

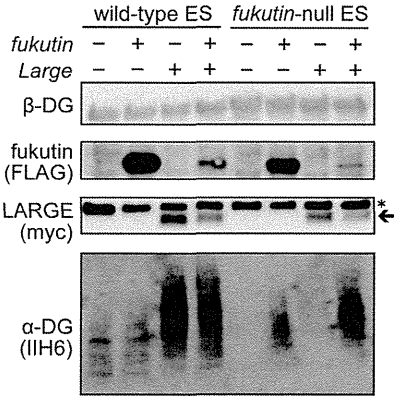

Figure 4 | α-DG glycosylation in *fukutin*-null ES cells after fukutin or LARGE expression. Fukutin (FLAG-tagged) and/or LARGE (myc-tagged) were expressed in wild-type or *fukutin*-null mouse ES cells and α-DG glycosylation status was analysed by western blotting. Exogenous LARGE expression produced highly glycosylated α-DG in wild-type but not *fukutin*-null ES cells, indicated by IIH6 staining. Co-transfection of *fukutin* and *Large* yielded LARGE-dependent glycosylation of α-DG in *fukutin*-null ES cells. Arrow and asterisk indicate LARGE protein and non-specific signals, respectively. The full-length blots with α-DG (IIH6), LARGE (myc), fukutin (FLAG), and β-DG are presented in Supplementary Figure S2i-l, respectively.

Protein preparation and western blotting. DG was enriched from solubilized skeletal muscle as described[27]. Briefly, skeletal muscles (TA ~30 mg, calf ~100 mg) were solubilised in Tris-buffered saline containing 1% Triton X-100 and protease inhibitors (Nacalai). The solubilised fraction was incubated with wheat germ agglutinin (WGA)-agarose beads (Vector Laboratories) at 4°C for 16 h; DG was eluted with SDS-PAGE loading buffer. To detect LARGE protein expression, total lysates were analysed by western blotting. Proteins were separated in 4–15% linear gradient SDS gels, then transferred to polyvinylidene fluoride (PVDF) membranes (Millipore). Blots were probed with antibodies and developed with horseradish peroxidase (HRP)-enhanced chemiluminescence reagent (Supersignal West Pico, Pierce; or ECL Prime, GE Healthcare).

Histology and immunofluorescence analysis. For H&E staining, cryosections (7 μm) were stained for 2 min in haematoxylin, 1 min in eosin, and dehydrated with ethanol and xylene. IIH6-immunofluorescence analysis was performed after treating the with cold ethanol/acetic acid (1 : 1) for 1 min, blocking with 5% goat serum in MOM Mouse Ig Blocking Reagent (Vector Laboratories) at room temperature for 1 h, and incubation with primary antibodies diluted in MOM Diluent (Vector Laboratories) overnight at 4°C. For F4/80- and collagen I-immunofluorescence, sections were blocked with 3% bovine serum albumin (BSA) in phosphate-buffered saline (PBS) at room temperature for 1 h, and then with primary antibodies diluted in 1% BSA overnight at 4°C. The slides were washed with PBS and incubated with Alexa Fluor 488-conjugated or Alexa Fluor 555-conjugated secondary antibodies (Molecular Probes) at room temperature for 30 min. Permount (Fisher Scientific) and TISSU MOUNT (Shiraimatsu Kikai) were used for H&E staining and immunofluorescence, respectively. Sections were observed by fluorescence microscopy (Leica DMR, Leica Microsystems).

ES cell culture. ES cells were cultured in DMEM with 20% heat-inactivated foetal bovine serum, 100 μM 2-mercaptoethanol, 1 mM non-essential amino acids (Gibco), 2 mM L-glutamine (Nacalai), and 10^3 U/mL leukaemia inhibitory factor (Millipore). Targeted disruptions of the *fukutin* gene in ES cells have been described previously[53]. Transfection was performed with Lipofectamine LTX reagents (Invitrogen) according to manufacturer protocols. After 48 h transfection, cells were lysed with Tris-buffered saline containing 1% Triton X-100 and protease inhibitors (Nacalai). DG proteins were enriched with WGA-beads and analysed by western blotting.

1. Toda, T. *et al.* Fukuyama-type congenital muscular dystrophy (FCMD) and alpha-dystroglycanopathy. *Congenit. Anom. (Kyoto).* **43**, 97–104 (2003).
2. Michele, D. E. & Campbell, K. P. Dystrophin-glycoprotein complex: post-translational processing and dystroglycan function. *J. Biol. Chem.* **278**, 15457–15460 (2003).
3. Beltrán-Valero de Bernabé, D. *et al.* Mutations in the O-mannosyltransferase gene POMT1 give rise to the severe neuronal migration disorder Walker-Warburg syndrome. *Am. J. Hum. Genet.* **71**, 1033–1043 (2002).

4. van Reeuwijk, J. *et al.* POMT2 mutations cause alpha-dystroglycan hypoglycosylation and Walker-Warburg syndrome. *J. Med. Genet.* **42**, 907–912 (2005).
5. Yoshida, A. *et al.* Muscular dystrophy and neuronal migration disorder caused by mutations in a glycosyltransferase, POMGnT1. *Dev. Cell* **1**, 717–724 (2001).
6. Kobayashi, K. *et al.* An ancient retrotransposal insertion causes Fukuyama-type congenital muscular dystrophy. *Nature* **394**, 388–392 (1998).
7. Brockington, M. *et al.* Mutations in the fukutin-related protein gene (FKRP) cause a form of congenital muscular dystrophy with secondary laminin alpha2 deficiency and abnormal glycosylation of alpha-dystroglycan. *Am. J. Hum. Genet.* **69**, 1198–1209 (2001).
8. Longman, C. *et al.* Mutations in the human LARGE gene cause MDC1D, a novel form of congenital muscular dystrophy with severe mental retardation and abnormal glycosylation of alpha-dystroglycan. *Hum. Mol. Genet.* **12**, 2853–2861 (2003).
9. Willer, T. *et al.* ISPD loss-of-function mutations disrupt dystroglycan O-mannosylation and cause Walker-Warburg syndrome. *Nat. Genet.* **44**, 575–580 (2012).
10. Roscioli, T. *et al.* Mutations in ISPD cause Walker-Warburg syndrome and defective glycosylation of α-dystroglycan. *Nat. Genet.* **44**, 581–585 (2012).
11. Manzini, M. C. *et al.* Exome sequencing and functional validation in zebrafish identify GTDC2 mutations as a cause of Walker-Warburg syndrome. *Am. J. Hum. Genet.* **91**, 541–517 (2012).
12. Hara, Y. *et al.* A dystroglycan mutation associated with limb-girdle muscular dystrophy. *N. Engl. J. Med.* **364**, 939–946 (2011).
13. Vuillaumier-Barrot, S. *et al.* Identification of mutations in TMEM5 and ISPD as a cause of severe cobblestone lissencephaly. *Am. J. Hum. Genet.* **91**, 1135–1143 (2012).
14. Jae, L. T. *et al.* Deciphering the glycosylome of dystroglycanopathies using haploid screens for lassa virus entry. *Science* **340**, 479–483 (2013).
15. Stevens, E. *et al.* Mutations in B3GALNT2 cause congenital muscular dystrophy and hypoglycosylation of α-dystroglycan. *Am. J. Hum. Genet.* **92**, 354–365 (2013).
16. Buysse, K. *et al.* Missense mutations in β-1,3-N-acetylglucosaminyltransferase 1 (B3GNT1) cause Walker-Warburg syndrome. *Hum. Mol. Genet.* **22**, 1746–1754 (2013).
17. Carss, K. J. *et al.* Mutations in GDP-mannose pyrophosphorylase B cause congenital and limb-girdle muscular dystrophies associated with hypoglycosylation of α-dystroglycan. *Am. J. Hum. Genet.* **93**, 29–41 (2013).
18. Lefeber, D. J. *et al.* Autosomal recessive dilated cardiomyopathy due to DOLK mutations results from abnormal dystroglycan O-mannosylation. *PLoS Genet.* **7**, e1002427 (2011).
19. Yang, A. C. *et al.* Congenital disorder of glycosylation due to DPM1 mutations presenting with dystroglycanopathy-type congenital muscular dystrophy. *Mol. Genet. Metab.* **110**, 345–351 (2013).
20. Barone, R. *et al.* DPM2-CDG: a muscular dystrophy-dystroglycanopathy syndrome with severe epilepsy. *Ann. Neurol.* **72**, 550–558 (2012).
21. Lefeber, D. J. *et al.* Deficiency of Dol-P-Man synthase subunit DPM3 bridges the congenital disorders of glycosylation with the dystroglycanopathies. *Am. J. Hum. Genet.* **85**, 76–86 (2009).
22. Kanagawa, M. Dystroglycan glycosylation and its involvement in muscular dystrophy. *Trends Glycosci. Glycotech.* **26**, 41–57 (2014).
23. Barresi, R. & Campbell, K. P. Dystroglycan: from biosynthesis to pathogenesis of human disease. *J. Cell Sci.* **119**, 199–207 (2006).
24. Yoshida-Moriguchi, T. *et al.* O-mannosyl phosphorylation of alpha-dystroglycan is required for laminin binding. *Science* **327**, 88–92 (2010).
25. Michele, D. E. *et al.* Post-translational disruption of dystroglycan-ligand interactions in congenital muscular dystrophies. *Nature* **418**, 417–422 (2002).
26. Han, R. *et al.* Basal lamina strengthens cell membrane integrity via the laminin G domain-binding motif of alpha-dystroglycan. *Proc. Natl. Acad. Sci. USA.* **106**, 12573–12579 (2009).
27. Kanagawa, M. *et al.* Impaired viability of muscle precursor cells in muscular dystrophy with glycosylation defects and amelioration of its severe phenotype by limited gene expression. *Hum. Mol. Genet.* **22**, 3003–3015 (2013).
28. Godfrey, C. *et al.* Refining genotype phenotype correlations in muscular dystrophies with defective glycosylation of dystroglycan. *Brain* **130**, 2725–2735 (2007).
29. Godfrey, C., Foley, A. R.., Clement, E. & Muntoni, F. Dystroglycanopathies: coming into focus. *Curr. Opin. Genet. Dev.* **21**, 278–285 (2011).
30. Murakami, T. *et al.* Fukutin gene mutations cause dilated cardiomyopathy with minimal muscle weakness. *Ann. Neurol.* **60**, 597–602 (2006).
31. Hayashi, Y. K. *et al.* Selective deficiency of alpha-dystroglycan in Fukuyama-type congenital muscular dystrophy. *Neurology* **57**, 115–121 (2001).
32. Fukuyama, Y., Osawa, M. & Suzuki, H. Congenital progressive muscular dystrophy of the Fukuyama type - clinical, genetic and pathological considerations. *Brain Dev.* **3**, 1–29 (1981).
33. Toda, T., Kobayashi, K., Kondo-Iida, E., Sasaki, J. & Nakamura, Y. The Fukuyama congenital muscular dystrophy story. *Neuromuscul. Disord.* **10**, 153–159 (2000).
34. Kuga, A. *et al.* Absence of post-phosphoryl modification in dystroglycanopathy mouse models and wild-type tissues expressing non-laminin binding form of α-dystroglycan. *J. Biol. Chem.* **287**, 9560–9567 (2012).
35. Inamori, K. *et al.* Dystroglycan function requires xylosyl- and glucuronyltransferase activities of LARGE. *Science* **335**, 93–96 (2012).
36. Goddeeris, M. M. *et al.* LARGE glycans on dystroglycan function as a tunable matrix scaffold to prevent dystrophy. *Nature* **503**, 136–140 (2013).
37. Barresi, R. *et al.* LARGE can functionally bypass alpha-dystroglycan glycosylation defects in distinct congenital muscular dystrophies. *Nat. Med.* **10**, 696–703 (2004).
38. Yu, M. *et al.* Adeno-associated viral-mediated LARGE gene therapy rescues the muscular dystrophic phenotype in mouse models of dystroglycanopathy. *Hum. Gene Ther.* **24**, 317–330 (2013).
39. Vannoy, C. H. *et al.* Adeno-associated virus-mediated overexpression of LARGE rescues α-dystroglycan function in dystrophic mice with mutations in the fukutin-related protein. *Hum. Gene. Ther. Methods.* **25**, 187–196 (2014).
40. Yagi, H. *et al.* AGO61-dependent GlcNAc modification primes the formation of functional glycans on α-dystroglycan. *Sci. Rep.* **3**, 3288 (2013).
41. Whitmore, C. *et al.* The transgenic expression of LARGE exacerbates the muscle phenotype of dystroglycanopathy mice. *Hum. Mol. Genet.* **23**, 1842–1855 (2014).
42. Saito, F. *et al.* Overexpression of LARGE suppresses muscle regeneration via down-regulation of insulin-like growth factor 1 and aggravates muscular dystrophy in mice. *Hum. Mol. Genet.* **23**, 4543–4558 (2014).
43. Gumerson, J. D. *et al.* Muscle-specific expression of LARGE restores neuromuscular transmission deficits in dystrophic LARGE(myd) mice. *Hum. Mol. Genet.* **22**, 757–768 (2013).
44. Yoshida-Moriguchi, T. *et al.* SGK196 is a glycosylation-specific O-mannose kinase required for dystroglycan function. *Science* **341**, 896–899 (2013).
45. Taniguchi-Ikeda, M. *et al.* Pathogenic exon-trapping by SVA retrotransposon and rescue in Fukuyama muscular dystrophy. *Nature* **478**, 127–131 (2011).
46. Kanagawa, M. *et al.* Residual laminin-binding activity and enhanced dystroglycan glycosylation by LARGE in novel model mice to dystroglycanopathy. *Hum. Mol. Genet.* **18**, 621–631 (2009).
47. Foust, K. D. *et al.* Intravascular AAV9 preferentially targets neonatal neurons and adult astrocytes. *Nat. Biotechnol.* **27**, 59–65 (2009).
48. Nakano, I., Funahashi, M., Takada, K. & Toda, T. Are breaches in the glia limitans the primary cause of the micropolygyria in Fukuyama-type congenital muscular dystrophy (FCMD)? Pathological study of the cerebral cortex of an FCMD fetus. *Acta. Neuropathol.* **91**, 313–321 (1996).
49. Chiyonobu, T. *et al.* Effects of fukutin deficiency in the developing mouse brain. *Neuromuscul. Disord.* **15**, 416–426 (2005).
50. Okada, T. *et al.* Scalable purification of adeno-associated virus serotype 1 (AAV1) and AAV8 vectors, using dual ion-exchange adsorptive membranes. *Hum. Gene Ther.* **20**, 1013–1021 (2009).
51. Yuasa, K. *et al.* Adeno-associated virus vector-mediated gene transfer into dystrophin-deficient skeletal muscles evokes enhanced immune response against the transgene product. *Gene Ther.* **9**, 1576–1588 (2002).
52. Kanagawa, M. *et al.* Post-translational maturation of dystroglycan is necessary for pikachurin binding and ribbon synaptic localization. *J. Biol. Chem.* **285**, 31208–31216 (2010).
53. Takeda, S. *et al.* Fukutin is required for maintenance of muscle integrity, cortical histiogenesis and normal eye development. *Hum. Mol. Genet.* **12**, 1449–1459 (2003).

Acknowledgments

We would like to thank the past and present members of Dr. Toda's laboratory for fruitful discussions and scientific contributions. We also thank Hiromi Hayashita-Kinoh for providing technical support. This work was supported by the Ministry of Health, Labour, and Welfare of Japan [Intramural Research Grant for Neurological and Psychiatric Disorders of National Centre of Neurology and Psychiatry (26-8)]; the Ministry of Education, Culture, Sports, Science and Technology of Japan [a Grant-in-Aid for Scientific Research (A) 26253057 to T.T.; a Grant-in-Aid for Young Scientists (A) 24687017 to M.K.; and a Grant-in-Aid for Scientific Research on Innovative Areas (Deciphering sugar chain-based signals regulating integrative neuronal functions) 24110508 to M.K.]; a Senri Life Science Foundation grant to M.K.; and a Takeda Science Foundation grant to M.K.

Author contributions

Y.O., M.K., T.O., K.K., S.T. and T.T. conceived and designed the research. Y.O., M.K. and C.I. performed experiments and analysed the data. C.Y., K.K., T.C. and T.O. constructed the AAV vectors. Y.O., M.K. and T.T. wrote the paper. All authors reviewed the manuscript.

Additional information

Supplementary information accompanies this paper at http://www.nature.com/scientificreports

Competing financial interests: The authors declare no competing financial interests.

How to cite this article: Ohtsuka, Y. *et al.* Fukutin is prerequisite to ameliorate muscular dystrophic phenotype by myofiber-selective LARGE expression. *Sci. Rep.* **5**, 8316; DOI:10.1038/srep08316 (2015).

REPORT

ERBB4 Mutations that Disrupt the Neuregulin-ErbB4 Pathway Cause Amyotrophic Lateral Sclerosis Type 19

Yuji Takahashi,[1] Yoko Fukuda,[1] Jun Yoshimura,[2] Atsushi Toyoda,[3] Kari Kurppa,[4,5] Hiroyoko Moritoyo,[6] Veronique V. Belzil,[7] Patrick A. Dion,[7,8] Koichiro Higasa,[2] Koichiro Doi,[2] Hiroyuki Ishiura,[1] Jun Mitsui,[1] Hidetoshi Date,[1] Budrul Ahsan,[1] Takashi Matsukawa,[1] Yaeko Ichikawa,[1] Takashi Moritoyo,[6] Mayumi Ikoma,[9] Tsukasa Hashimoto,[9] Fumiharu Kimura,[10] Shigeo Murayama,[11] Osamu Onodera,[12] Masatoyo Nishizawa,[12] Mari Yoshida,[13] Naoki Atsuta,[14] Gen Sobue,[14] JaCALS,[15] Jennifer A. Fifita,[16,17,18] Kelly L. Williams,[16,17,18] Ian P. Blair,[16,17,18] Garth A. Nicholson,[16,17] Paloma Gonzalez-Perez,[19] Robert H. Brown, Jr.,[19] Masahiro Nomoto,[6] Klaus Elenius,[4,20] Guy A. Rouleau,[7,21,22] Asao Fujiyama,[3] Shinichi Morishita,[2] Jun Goto,[1] and Shoji Tsuji[1,23,*]

Amyotrophic lateral sclerosis (ALS) is a devastating neurological disorder characterized by the degeneration of motor neurons and typically results in death within 3–5 years from onset. Familial ALS (FALS) comprises 5%–10% of ALS cases, and the identification of genes associated with FALS is indispensable to elucidating the molecular pathogenesis. We identified a Japanese family affected by late-onset, autosomal-dominant ALS in which mutations in genes known to be associated with FALS were excluded. A whole- genome sequencing and parametric linkage analysis under the assumption of an autosomal-dominant mode of inheritance with incomplete penetrance revealed the mutation c.2780G>A (p. Arg927Gln) in *ERBB4*. An extensive mutational analysis revealed the same mutation in a Canadian individual with familial ALS and a de novo mutation, c.3823C>T (p. Arg1275Trp), in a Japanese simplex case. These amino acid substitutions involve amino acids highly conserved among species, are predicted as probably damaging, and are located within a tyrosine kinase domain (p. Arg927Gln) or a C-terminal domain (p. Arg1275Trp), both of which mediate essential functions of ErbB4 as a receptor tyrosine kinase. Functional analysis revealed that these mutations led to a reduced autophosphorylation of ErbB4 upon neuregulin-1 (NRG-1) stimulation. Clinical presentations of the individuals with mutations were characterized by the involvement of both upper and lower motor neurons, a lack of obvious cognitive dysfunction, and relatively slow progression. This study indicates that disruption of the neuregulin-ErbB4 pathway is involved in the pathogenesis of ALS and potentially paves the way for the development of innovative therapeutic strategies such using NRGs or their agonists to upregulate ErbB4 functions.

Amyotrophic lateral sclerosis (ALS) is a devastating neurological disorder in which the degeneration of motor neurons leads to progressive weakness and wasting of limb, bulbar, and respiratory muscles. Familial ALS (FALS) comprises 5%–10% of ALS cases, and the remaining cases are simplex cases of ALS (SALS). To date, more than 20 genes have been shown to be associated with ALS,[1] and these account for 75% of FALS and 14% of SALS cases.[2] Mutations that are found in FALS-associated genes but that are also identified in individuals with SALS are considered mutations with reduced penetrance or de novo mutations. Further discovery of genes associated with FALS is indispensable to elucidating the molecular backgrounds of both FALS and SALS.

Identification of genes associated with familial diseases has been accomplished through identification of the disease loci on the chromosomes by linkage analysis of large pedigrees and subsequent positional cloning of the genes. The majority of the FALS pedigrees, however, are not large and do not have multiple affected members as a result of the poor prognosis of the disease and the late age of onset, which makes it difficult to sufficiently narrow the candidate regions by linkage analyses and means that it takes a tremendous effort to identify the genes associated with FALS. The recent development of massively parallel

[1]Department of Neurology, Graduate School of Medicine, The University of Tokyo, Tokyo 113-8655, Japan; [2]Department of Computational Biology, Graduate School of Frontier Sciences, The University of Tokyo, Chiba 277-8561, Japan; [3]Comparative Genomics Laboratory, National Institute of Genetics, Shizuoka 411-8540, Japan; [4]Department of Medical Biochemistry and Genetics, University of Turku, Turku, 20014, Finland; [5]Turku Doctoral Programme of Biomedical Sciences, Turku, 20520, Finland; [6]Department of Neurology and Clinical Pharmacology, Ehime University Hospital, Ehime 791-0295, Japan; [7]Research Center, Centre Hospitalier Universitaire Sainte-Justine, Université de Montreal, Montreal, QC, H3T 1C5, Canada; [8]Department of Pathology and Cellular Biology, Université de Montréal, Montreal, QC H3T 1C5, Canada; [9]Department of Neurology, National Hospital Organization Ehime National Hospital, Ehime 791-0281, Japan; [10]Division of Neurology, First Department of Internal Medicine, Osaka Medical College, Osaka 569-8686, Japan; [11]Department of Neurology and Neuropathology and Brain Bank for Aging Research, Tokyo Metropolitan Geriatric Hospital and Institute of Gerontology, Tokyo 173-0015, Japan; [12]Department of Neurology, Brain Research Institute, Niigata University, Niigata 951-8520, Japan; [13]Department of Neuropathology, Institute for Medical Science of Aging, Aichi Medical University, Aichi 480-1195, Japan; [14]Department of Neurology, Nagoya University Graduate School of Medicine, Nagoya 466-8560, Japan; [15]Japanese Consortium for Amyotrophic Lateral Sclerosis Research; [16]Northcott Neuroscience Laboratory, ANZAC Research Institute, Sydney, New South Wales 2139, Australia; [17]Sydney Medical School, University of Sydney, New South Wales 2006, Australia; [18]Austrian School of Medicine, Macquarie University, Sydney, New South Wales 2109, Australia; [19]Department of Neurology, University of Massachusetts Medical School, Worcester, MA 01655-0318, USA; [20]Department of Oncology, Turku University Hospital, Turku 20521, Finland; [21]Montreal Neurological Institute, McGill University, Montreal, QC H3A 2B4, Canada; [22]Department of Neurology and Neurosurgery, McGill University, Montreal, QC H3A 2B4, Canada; [23]Medical Genome Center, The University of Tokyo Hospital, The University of Tokyo, Tokyo 113-8655, Japan
*Correspondence: tsuji@m.u-tokyo.ac.jp
http://dx.doi.org/10.1016/j.ajhg.2013.09.008.

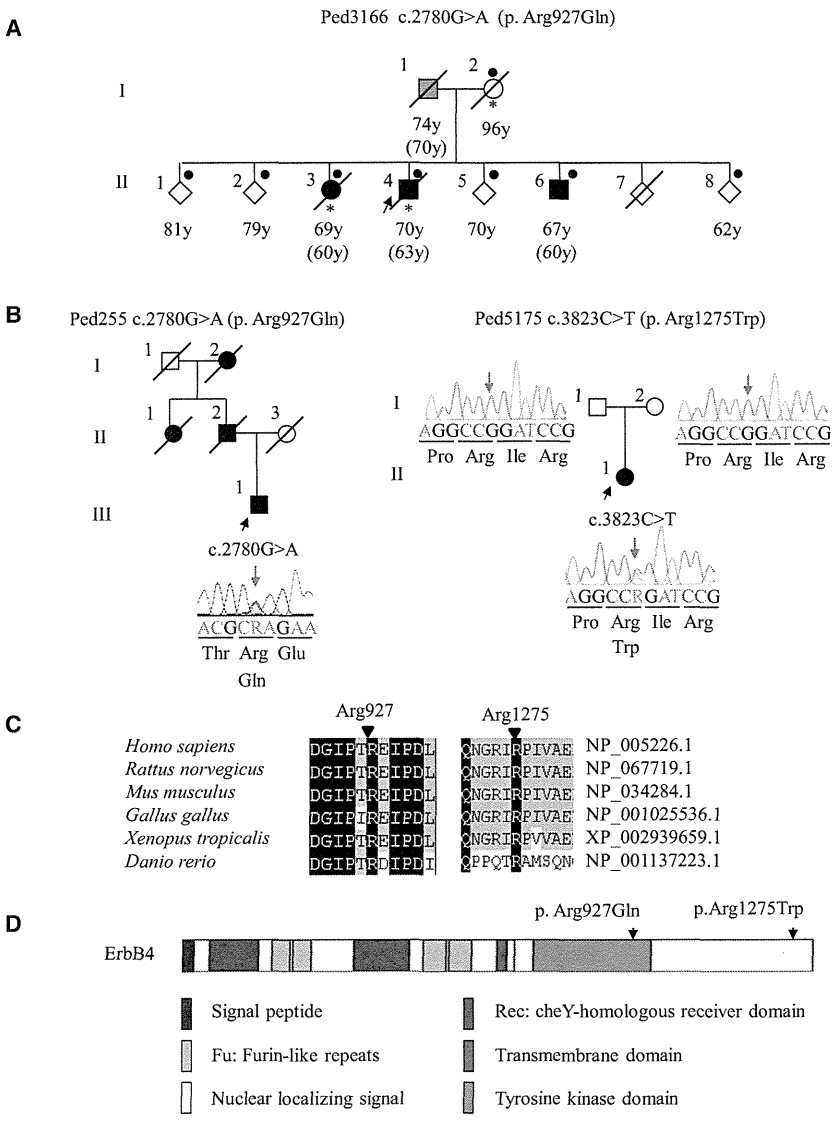

Figure 1. Pedigrees of ALS and Characterization of Mutations

(A) Pedigree charts of the index family. Filled symbols indicate affected individuals. The arrow indicates the proband. For confidentiality purposes, all unaffected siblings are indicated by diamonds. Dots or asterisks indicate individuals included in the linkage study or WGS, respectively. Age at present or age at death is shown under each individual, and ages at onset are shown in parentheses. The box with gray shading indicates that the individual's clinical information obtained from the family members strongly supports the diagnosis of ALS, although detailed neurological evaluations have not been conducted for this individual.

(B) Additional Canadian (Ped255) and Japanese (Ped5175) pedigrees with *ERBB4* mutations. The electropherograms of mutational data are shown beside each member. Nucleotide colors correspond to the colors in the electropherograms. The amino acids are designated below the nucleotide sequences. The blue arrows indicate the nucleotide positions of the mutations. In the electropherograms (Ped5175), nucleotide sequences of the reverse complementary strand are shown.

(C) Amino acid conservation. The amino acids Arg927 and Arg1275 are highly conserved among species.

(D) The protein structure along with the locations of amino acid substitutions are shown; amino acid substitutions are indicated by arrows. The amino acid substitution p. Arg927Gln resides in the tyrosine kinase domain, which mediates the key functions of ErbB4. The amino acid substitution p. Arg1275Trp resides in the C-terminal domain in the vicinity of multiple phosphorylation sites, which mediate downstream signaling pathways.

sequencing technologies has allowed us to overcome the difficulty by means of whole-genome sequencing (WGS) or exome analysis.

We identified a Japanese family with three affected siblings presenting with late-onset ALS (Figure 1A and Table 1). The familial history indicated that the mode of inheritance is probably an autosomal-dominant one. Mutational analysis of the proband (II-4) employing direct nucleotide sequence analysis, a microarray-based resequencing, or a repeat-primed PCR analysis excluded *SOD1*[MIM 147450], *ALS2*[MIM 606352], *DCTN1*[MIM 601143], *CHMP2B*[MIM 609512], *ANG*[MIM 105850], *TARDBP*[MIM 605078], *FUS*[MIM 137070] and *C9ORF72* [MIM 1614260] as the genes associated with FALS.[3,4] To identify a gene associated with FALS, we applied WGS in combination with a linkage analysis to the pedigree. Written informed consent was obtained from all the participants. This study was approved by the institutional review board at the University of Tokyo.

WGS was performed on three individuals (I-2, II-3 and II-4, as shown in Figure 1A) in the index pedigree. Paired-end DNA libraries were generated and subjected to massively parallel sequencing with a GAII Illumina Genome Analyzer in accordance with the manufacturer's instructions. The short read sequences obtained were aligned to the reference genome (NCBI37/hg19 assembly) via the Burrows-Wheeler Aligner.[5] Downstream analyses in which potential PCR duplicates were removed were processed with SAMtools.[6] Aligned reads were viewed on an Integrative Genomics Viewer.[7] Genomic sequence variations were identified with the SAMtools pileup command and annotated with Refseq, dbSNP135, 1000 Genomes, personal genome databases, the NHLBI GO Exome Sequencing Project (NHLBI-ESP) database, and an in-house variant database containing 41 whole genomes and 1,408 exomes in the Japanese population. The numbers of nonsynonymous variants that were identified in individuals I-2, II-3, and II-4 but that were not present in any of the

Table 1. Clinical Characteristics of Affected Individuals

Pedigree Number	Pedigree 3166				Pedigree 255	Pedigree 5175
Ethnicity	Japanese				Canadian	Japanese
Inheritance	familial (autosomal dominant)				familial (autosomal dominant)	simplex
Mutation	c.2780G>A				c.2780G>A	c.3823C>T
Amino acid substitution	p. Arg927Gln				p. Arg927Gln	p. Arg1275Trp
Members	I-1	II-3	II-4 (proband)	II-6	III-3	II-1
Age at onset	70	60	63	60	67	45
Initial symptoms	bulbar	N.D.	upper limbs	respiration	upper limbs	upper limbs
Diagnostic criteria[a]	N.D.	N.D.	definite	definite	probable	probable
Progression	unable to walk after 3 years	ventilator -dependent after 5 years, locked-in state after 8 years	locked-in state after 5 years	ventilator- dependent after 1 year, locked-in state after 5 years	slow progression that significantly decelerated and finally stopped after 8 years	wheelchair- bound, MRS 1-2/5 in upper extremities after 5 years
Cognitive function	N.D.	N.D.	normal	normal	N.D.	normal
Age at death	74	69	70	66	N/A	N/A

Abbreviations are as follows: N.D., not described; MRS, manual muscle testing rating scale; and N/A, not applicable.
[a]El Escorial and Airlie House revised criteria.

databases (hereafter, variants not found in the databases are referred to as "novel") were 411, 404, and 382, respectively (Table S1). No novel nonsynonymous variants in genes known to be associated with FALS were included. Among the identified variants, 57 were identified both in the proband and in the affected sibling, but not in the mother, and were subjected to further analysis.

The individuals indicated by dots in Figure 1A were genotyped with Genome-Wide Human SNP Array 6.0 (Affymetrix). Linkage analysis and haplotype reconstruction were conducted with the pipeline software SNP-HiTLink[8] and Allegro version 2[9] under the assumption of an autosomal-dominant mode of inheritance and a disease-allele frequency of 0.000001. Parametric multipoint linkage analysis under the assumption of complete penetrance revealed three loci spanning 23.6 Mb on chromosomes 1, 6, and 13, having a maximum LOD score of 1.8 (Figure S1; penetrance = 1.0), and containing 88 annotated genes. However, no novel nonsynonymous variants were identified in the candidate regions. We then considered the possibility of reduced penetrance. When penetrance was reduced to 0.8 (Figure S1), seven additional loci had LOD scores > 0.7 and were thus shown to support linkage; these loci contained 809 annotated genes. Three heterozygous novel nonsynonymous variants were identified in these regions; among these variants, only c.2780G>A (p. Arg927Gln; dbSNP SubSNP ID ss831884245) substituting glutamine for arginine at codon 927 (p. Arg927Gln) in v-erb-a erythroblastic leukemia viral oncogene homolog 4 (avian) (*ERBB4* [MIM 600543; RefSeq accession number NM_005235.2]) was not present in 477 controls (Table S2). When we allowed further reduced penetrance, we identified 19 additional loci with LOD > 0; these loci contained 1,265 annotated genes. In these regions, we identified seven heterozygous novel nonsynonymous variants, among which three variants in *OR2D3* (RefSeq NM_001004684.1), *FTCD* (MIM 606806; RefSeq NM_206965.1), and *TJP2* (MIM 607709; RefSeq NM_001170414.2) were not present in 477 controls (Table S2). *OR2D3* is an olfactory receptor gene; the substituted amino acid in *OR2D3* is not conserved, and the substitution is predicted as benign by PolyPhen-2 analysis. *FTCD* and *TJP2* are associated with autosomal-recessive glutamate formiminotransferase deficiency (MIM 229100) and familial hypercholanemia (MIM 607748), respectively, and heterozygous carriers have not been described as exhibiting ALS. Taken together, the results pointed to c.2780G>A in *ERBB4* as the most likely pathogenic mutation.

We used a direct nucleotide sequence analysis method to conduct mutational analysis of *ERBB4* in 364 FALS and 818 SALS individuals by using an ABI 3100 sequencer and BigDye Terminator ver3.1 (Applied Biosystems). We used the ExonPrimer website to design oligonucleotide primers (Table S3). The mutation c.2780G>A was also identified in one Canadian FALS individual (Figure 1B). Unfortunately, DNA from other family members was not available to confirm segregation. To investigate a possibility that the c.2780G>A mutation identified in the Japanese and Canadian families is a common founder mutation, we compared the haplotypes with the c.2780G>A mutation in *ERBB4* of the Japanese and Canadian families (Figure S2). Different SNPs were observed 14 kbp and 5 kbp centromeric and telomeric to the mutation, respectively, indicating that disease haplotypes of the Japanese and Canadian families are different and that

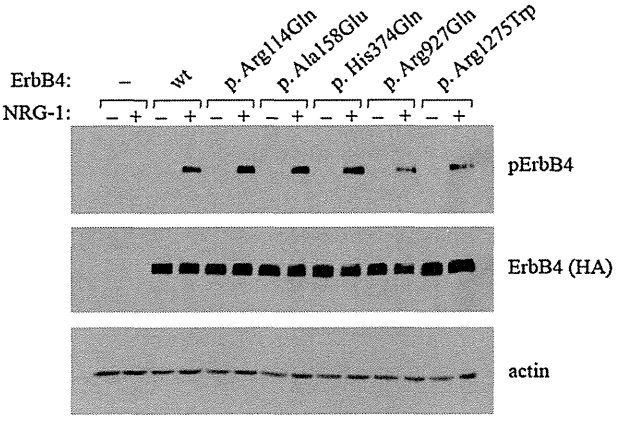

Figure 2. Functional Analysis of Wild-Type and Mutant ErbB4 upon Neuregulin-1 Stimulation
COS-7 cells transfected with an empty-vector control or plasmids encoding either wild-type (wt) or mutant HA-tagged ErbB4 (p. Arg114Gln, p. Ala158Glu, p. His374Gln, p. Arg927Gln, or p. Arg1275Trp) were stimulated with or without NRG-1, and the autophosphorylation activity of ErbB4 was analyzed by immunoblot analysis with antibodies against phospho-ErbB4 (Tyr1284) (Cell Signaling) and HA tag (Abcam), respectively. For loading controls, immunoblotting was performed with an anti-actin antibody (Santa Cruz Biotechnology). Three amino acid substitutions, including p.Arg114Gln, p.Ala158Glu, and p.His374Gln (rs760369), identified through mutational analysis of FALS and SALS individuals, were included in autophosphorylation assay. The substitutions p.Arg114Gln and p.Ala158Glu were not considered to be relevant to ALS because neither recurrence nor cosegregation was confirmed.

mutation occurred independently. We identified a de novo mutation of c.3823C>T (dbSNP SubSNP ID ss831884246), substituting tryptophan for arginine at codon 1275 (p. Arg1275Trp), in a Japanese SALS individual (Figure 1B) in whom a biological parent-descendant relationship was confirmed (Table S4) by the PLINK[10] algorithm. These mutations were neither present in the 477 Japanese controls nor registered in the in-house database containing 41 whole genomes and 1408 exomes, the 1000 Genomes database, or the NHLBI-ESP database, containing 6503 exomes. Furthermore, c.2780G>A was not present in 190 Canadian controls. The identification of c.2780G>A in two independent families of different ethnic backgrounds strongly supported c.2780G>A as the causative mutation for ALS. Given that de novo mutation rates have been estimated to be 1.20×10^{-8} per nucleotide per generation[11] and less than one nonsynonymous single-nucleotide variant (SNV)/generation,[12] the observation of the de novo mutation further supports the idea that c.3823C>T is likely to be the causative mutation for ALS in this individual. The mutation's substituted arginine residues, Arg927 and Arg1275, are highly conserved among species (Figure 1C), and the substitutions are predicted to be probably damaging by PolyPhen-2 analysis. The amino acid residue Arg927 resides in a tyrosine kinase domain, which is essential for the receptor tyrosine kinase activity, and Arg1275 is located in a C-terminal domain in the vicinity of multiple phosphorylation sites, which mediate downstream signaling pathways (Figure 1D). The clinical presentations of these ALS individuals with the *ERBB4* mutations are summarized in Table 1. The common clinical characteristics of the individuals included both upper and lower motor-neuron involvement diagnosed as definite or probable ALS according to El Escorial and Airlie House revised criteria, relatively slow disease progression, and no obvious cognitive impairment. The individuals with the c.2780G>A mutation were characterized by relatively late onset (the ages at onset ranged from 60–70 years) and a slightly reduced penetrance. In contrast, the individual with the c.3823C>T mutation was characterized by early onset (45 years of age).

ErbB4 is a member of the epidermal growth factor (EGF) subfamily of receptor tyrosine kinases (RTKs). It forms a homodimer or a heterodimer with ErbB2 or ErbB3 and is activated upon binding of neuregulins (NRGs) to the extracellular ligand-binding domain of ErbB4.[13] Activation of ErbB4 is mediated by increased tyrosine kinase activity upon NRG binding, resulting in autophosphorylation of the C-terminal tail.[14] To determine how the two mutations identified in the ALS individuals affect ErbB4 functions, we investigated the autophosphorylation of ErbB4 in cells expressing either wild-type or mutant (c.2780G>A or c.3823C>T) *ERBB4* in the presence of NRG-1. The *ERBB4* mutations were introduced into the pBABE-puro*ERBB4JM-aCYT-2HA* plasmid encoding HA-tagged ErbB4 JM-a CYT-2[15] by site-directed mutagenesis according to the protocol described in the Phusion Site-Directed Mutagenesis Kit (Thermo Fisher Scientific). After mutagenesis, all the constructs were verified by sequencing. The plasmids were transiently transfected into COS-7 cells via FuGENE 6 transfection reagent (Roche) in accordance with the manufacturer's instructions. Transfected cells were starved of serum overnight and stimulated with 0 or 50 ng/ml NRG-1 (R&D Systems) for 10 min at 37°C. After stimulation, the cells were lysed, and samples equivalent to 50 μg of total protein were separated through 8% SDS-PAGE gels. For detectiin of ErbB4 phosphorylation and total ErbB4 protein levels, immunoblotting was performed antibodies against phospho-ErbB4 (Tyr1284) (Cell Signaling) and HA-tag (Abcam), respectively. The two amino acid substitutions, p. Arg927Gln and p. Arg1275Trp, showed a clearly reduced autophosphorylation of ErbB4 (Figure 2). On the basis of these genetic and functional data, we concluded that the two mutations are causative mutations for ALS (ALS19).

This study revealed that a reduced autophosphorylation of ErbB4 upon NRG-1 stimulation is involved in the pathogenesis of ALS. *Erbb4* is specifically expressed in the soma of large motor neurons of the rat spinal cord.[16] The lack of *Erbb4* is embryonically lethal in mice, which displayed the derangement of motor-neuron axon guidance and pathfinding during embryogenesis.[17] Heterozygous-null mice showed a reduced body weight and delayed motor development, and brain-specific conditional knock-out mice

demonstrated reduced spontaneous motor activity and grip strength of the hindlimbs.[18] Mice lacking cysteine-rich domain (CRD) isoforms of *Nrg-1* (*CRD-NRG-1*$^{-/-}$) die perinatally as a result of respiratory failure, lack detectable limb movement, and exhibit a loss of ~60% of spinal motor neurons.[19] Similarly, motor and sensory neuron-specific conditional *Nrg-1* knockout mice die at birth and showed marked retraction of motor-neuron axons.[20] Furthermore, a decrease in the amount of CRD-NRG-1 has been detected in the spinal motor neurons in FALS and SALS individuals and *Sod1* mutant mice at disease onset,[21] raising the possibility that disruption of the NRG-ErbB pathway is commonly involved in the motor-neuron degeneration underlying ALS. This study provides insight into ALS pathogenesis and is expected to pave the way for the development of innovative therapeutic strategies such as using NRGs or their agonists to upregulate ErbB4 functions.

Supplemental Data

Supplemental Data include two figures and four tables and can be found with this article online at http://www.cell.com/AJHG/.

Consortia

Consortium members of JaCALS include Ryoichi Nakamura, Hazuki Watanabe, Yuishin Izumi, Ryuji Kaji, Mitsuya Morita, Kotaro Ogaki, Akira Taniguchi, Ikuko Aiba, Koichi Mizoguchi, Koichi Okamoto, Kazuko Hasegawa, Masashi Aoki, Akihiro Kawata, Imaharu Nakano, Koji Abe, Masaya Oda, Masaaki Konagaya, Takashi Imai, Masanori Nakagawa, Takuji Fujita, Hidenao Sasaki, and Masatoyo Nishizawa.

Acknowledgments

We thank all the family members for participating in this study. This study was supported in part by KAKENHI (Grants-in-Aid for Scientific Research on Innovative Areas [22129001 and 22129002]) to S.T.; the Global COE Program from the Ministry of Education, Culture, Sports, Science, and Technology of Japan, and a grant-in-aid (H23-Jitsuyoka [Nanbyo]-Ippan-004) from the Ministry of Health, Labour, and Welfare, Japan to S.T. We acknowledge support to R.H.B. from ALS Therapy Alliance, Project ALS, P2ALS, the Angel Fund, the Pierre L. de Bourgknecht ALS Research Foundation, the Al-Athel ALS Research Foundation, the ALS Family Charitable Foundation, and grant 1R01NS050557 from the National Institute of Neurological Disorders and Stroke of the National Institutes of Health and support to G.A.N. from the MND Research Institute of Australia. P.G.-P. was supported by the Alfonso Martin Escudero Foundation (Madrid).

Received: May 12, 2013
Revised: August 26, 2013
Accepted: September 13, 2013
Published: October 10, 2013

Web Resources

The URLs for data presented herein are as follows:

1000 Genomes Project Database, http://www.1000genomes.org/
dbSNP135, http://www.ncbi.nlm.nih.gov/projects/SNP/
ExonPrimer, http://ihg.gsf.de/ihg/ExonPrimer.html
NCBI37/hg19 assembly, http://genome.ucsc.edu/
NHLBI GO Exome Sequencing Project (NHLBI-ESP), https://esp.gs.washington.edu/drupal
Online Mendelian Inheritance in Man (OMIM), http://www.omim.org/
Personal genome databases, http://www.sequenceontology.org/resources/10Gen.html
PLINK algorithm, http://pngu.mgh.harvard.edu/purcell/plink/
PolyPhen-2, http://genetics.bwh.harvard.edu/pph2/
Refseq, http://www.ncbi.nlm.nih.gov/projects/RefSeq/
UCSC Human Genome Browser, http://genome.ucsc.edu/

Accession Numbers

The dbSNP accession numbers for the c. 2780G>A and c. 3823C>T mutations reported for *ERBB4* in this paper are ss831884245 and ss831884246, respectively.

References

1. Al-Chalabi, A., Jones, A., Troakes, C., King, A., Al-Sarraj, S., and van den Berg, L.H. (2012). The genetics and neuropathology of amyotrophic lateral sclerosis. Acta Neuropathol. *124*, 339–352.
2. Andersen, P.M., and Al-Chalabi, A. (2011). Clinical genetics of amyotrophic lateral sclerosis: what do we really know? Nat Rev Neurol *7*, 603–615.
3. Takahashi, Y., Seki, N., Ishiura, H., Mitsui, J., Matsukawa, T., Kishino, A., Onodera, O., Aoki, M., Shimozawa, N., Murayama, S., et al. (2008). Development of a high-throughput microarray-based resequencing system for neurological disorders and its application to molecular genetics of amyotrophic lateral sclerosis. Arch. Neurol. *65*, 1326–1332.
4. Ishiura, H., Takahashi, Y., Mitsui, J., Yoshida, S., Kihira, T., Kokubo, Y., Kuzuhara, S., Ranum, L.P., Tamaoki, T., Ichikawa, Y., et al. (2012). C9ORF72 repeat expansion in amyotrophic lateral sclerosis in the Kii peninsula of Japan. Arch. Neurol. *69*, 1154–1158.
5. Li, H., and Durbin, R. (2009). Fast and accurate short read alignment with Burrows-Wheeler transform. Bioinformatics *25*, 1754–1760.
6. Li, H., Handsaker, B., Wysoker, A., Fennell, T., Ruan, J., Homer, N., Marth, G., Abecasis, G., and Durbin, R.; 1000 Genome Project Data Processing Subgroup. (2009). The Sequence Alignment/Map format and SAMtools. Bioinformatics *25*, 2078–2079.
7. Robinson, J.T., Thorvaldsdóttir, H., Winckler, W., Guttman, M., Lander, E.S., Getz, G., and Mesirov, J.P. (2011). Integrative genomics viewer. Nat. Biotechnol. *29*, 24–26.
8. Fukuda, Y., Nakahara, Y., Date, H., Takahashi, Y., Goto, J., Miyashita, A., Kuwano, R., Adachi, H., Nakamura, E., and Tsuji, S. (2009). SNP HiTLink: a high-throughput linkage analysis system employing dense SNP data. BMC Bioinformatics *10*, 121.
9. Gudbjartsson, D.F., Thorvaldsson, T., Kong, A., Gunnarsson, G., and Ingolfsdottir, A. (2005). Allegro version 2. Nat. Genet. *37*, 1015–1016.
10. Purcell, S., Neale, B., Todd-Brown, K., Thomas, L., Ferreira, M.A., Bender, D., Maller, J., Sklar, P., de Bakker, P.I., Daly, M.J., and Sham, P.C. (2007). PLINK: a tool set for whole-genome association and population-based linkage analyses. Am. J. Hum. Genet. *81*, 559–575.

11. Kong, A., Frigge, M.L., Masson, G., Besenbacher, S., Sulem, P., Magnusson, G., Gudjonsson, S.A., Sigurdsson, A., Jonasdottir, A., Jonasdottir, A., et al. (2012). Rate of de novo mutations and the importance of father's age to disease risk. Nature *488*, 471–475.
12. Sanders, S.J., Murtha, M.T., Gupta, A.R., Murdoch, J.D., Raubeson, M.J., Willsey, A.J., Ercan-Sencicek, A.G., DiLullo, N.M., Parikshak, N.N., Stein, J.L., et al. (2012). De novo mutations revealed by whole-exome sequencing are strongly associated with autism. Nature *485*, 237–241.
13. Plowman, G.D., Green, J.M., Culouscou, J.M., Carlton, G.W., Rothwell, V.M., and Buckley, S. (1993). Heregulin induces tyrosine phosphorylation of HER4/p180erbB4. Nature *366*, 473–475.
14. Carpenter, G. (2003). ErbB-4: mechanism of action and biology. Exp. Cell Res. *284*, 66–77.
15. Sundvall, M., Korhonen, A., Vaparanta, K., Anckar, J., Halkilahti, K., Salah, Z., Aqeilan, R.I., Palvimo, J.J., Sistonen, L., and Elenius, K. (2012). Protein inhibitor of activated STAT3 (PIAS3) protein promotes SUMOylation and nuclear sequestration of the intracellular domain of ErbB4 protein. J. Biol. Chem. *287*, 23216–23226.
16. Pearson, R.J., Jr., and Carroll, S.L. (2004). ErbB transmembrane tyrosine kinase receptors are expressed by sensory and motor neurons projecting into sciatic nerve. J. Histochem. Cytochem. *52*, 1299–1311.
17. Gassmann, M., Casagranda, F., Orioli, D., Simon, H., Lai, C., Klein, R., and Lemke, G. (1995). Aberrant neural and cardiac development in mice lacking the ErbB4 neuregulin receptor. Nature *378*, 390–394.
18. Golub, M.S., Germann, S.L., and Lloyd, K.C.K. (2004). Behavioral characteristics of a nervous system-specific erbB4 knockout mouse. Behav. Brain Res. *153*, 159–170.
19. Wolpowitz, D., Mason, T.B., Dietrich, P., Mendelsohn, M., Talmage, D.A., and Role, L.W. (2000). Cysteine-rich domain isoforms of the neuregulin-1 gene are required for maintenance of peripheral synapses. Neuron *25*, 79–91.
20. Yang, X., Arber, S., William, C., Li, L., Tanabe, Y., Jessell, T.M., Birchmeier, C., and Burden, S.J. (2001). Patterning of muscle acetylcholine receptor gene expression in the absence of motor innervation. Neuron *30*, 399–410.
21. Song, F., Chiang, P., Wang, J., Ravits, J., and Loeb, J.A. (2012). Aberrant neuregulin 1 signaling in amyotrophic lateral sclerosis. J. Neuropathol. Exp. Neurol. *71*, 104–115.

J Neurol (2013) 260:2917–2927
DOI 10.1007/s00415-013-7112-y

Amyotrophic lateral sclerosis: an update on recent genetic insights

Yohei Iguchi · Masahisa Katsuno · Kensuke Ikenaka · Shinsuke Ishigaki · Gen Sobue

Received: 31 August 2013 / Revised: 10 September 2013 / Accepted: 12 September 2013 / Published online: 2 October 2013

Abstract Amyotrophic lateral sclerosis (ALS) is a devastating neurodegenerative disease affecting both upper and lower motor neurons. The prognosis for ALS is extremely poor, but there is a limited course of treatment with only one approved medication. A most striking recent discovery is that TDP-43 is identified as a key molecule that is associated with both sporadic and familial forms of ALS. TDP-43 is not only a pathological hallmark, but also a genetic cause for ALS. Subsequently, a number of ALS-causative genes have been found. Above all, the RNA-binding protein, such as FUS, TAF15, EWSR1 and hnRNPA1, have structural and functional similarities to TDP-43, and physiological functions of some molecules, including *VCP, UBQLN2, OPTN, FIG4* and *SQSTM1,* are involved in a protein degradation system. These discoveries provide valuable insight into the pathogenesis of ALS, and open doors for developing an effective disease-modifying therapy.

Keywords Amyotrophic lateral sclerosis · Motor neuron disease · Protein aggregation · RNA metabolism

Y. Iguchi · M. Katsuno · K. Ikenaka · S. Ishigaki · G. Sobue (✉)
Department of Neurology, Nagoya University Graduate School of Medicine, 65 Tsurumai-cho, Showa-ku, Nagoya 466-8550, Japan
e-mail: sobueg@med.nagoya-u.ac.jp

Y. Iguchi
The Centre de Recherche de l'Institut Universitaire en Santé Mentale de Québec-CRIUSMQ, Laval University, Quebec, QC G1J 2G3, Canada

Introduction

Amyotrophic lateral sclerosis (ALS) is an adult-onset, progressive, and devastating neurodegenerative disease. The typical ALS case develops a muscle weakness and atrophy, which result from selective motor neuronal death in the cortex, brain stem, and spinal cord, but does not affect the oculomotor, sensory or autonomic functions. ALS occurs alone or with frontotemporal lobar degeneration (FTLD). Transactive response (TAR)-DNA binding protein 43 kDa (TDP-43) was identified as a component of the ubiquitinated neuronal inclusion in sporadic ALS (SALS) and FTLD with ubiquitinated inclusions [1–3]. These two diseases have been regarded as part of the spectrum of a single disease referred to as TDP-43 proteinopathy. TDP-43 is reported to be a causative molecule of familial ALS (FALS) [4–7]. Subsequently, a number of ALS-causative genes have been identified (http://neuromuscular.wustl.edu/index.html). Some of the identified ALS-causative molecules share physiological roles indispensable for a cellular activity and are involved in SALS pathologies (Fig. 1). Although the cause of SALS, which accounts for ~90 % of ALS, is uncertain, these discoveries have provided novel insights into the pathogenesis of ALS. Here we review recent genetic findings concering ALS.

TARDBP

In 2006, two groups reported that TDP-43 is a major component of ubiquitinated neuronal cytoplasmic inclusions in both SALS and FTLD [1, 2]. In addition, mutations of *TARDBP,* the gene encoding TDP-43, cause an autosomal dominant FALS, which accounts for ~5 % of FALS

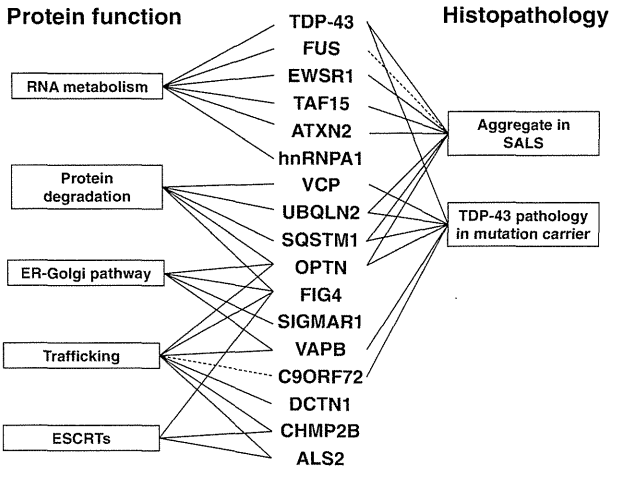

Fig. 1 Physiological and neuropathological overlaps of ALS-causative genes. Several ALS-causing molecules share similar cellular functions and are possibly co-localized in intra-neuronal aggregates of ALS. Aggregate in SALS; the protein encoded by each gene forms aggregates in a SALS-affected region. TDP-43 pathology in mutation carrier; TDP-43-positive cytoplasmic inclusion is observed in ALS cases with each mutation. ESCRTs, endosomal sorting complexes required for transport

cases [4–7]. Except for D169G, all *TARDBP* mutations are in the C-terminal glycine-rich region encoded by exon 6. Although ALS patients carrying TDP-43 mutations normally exhibit a classical ALS phenotype with rare co-occurrence of dementia, there is a trend for disease onset to be earlier, with upper limb onset being more common and a longer duration compared to SALS patients [8]. TDP-43 is an RNA-binding protein that regulates elements of RNA metabolism such as gene transcription, stability of mRNA, pre-mRNA splicing, and microRNA biogenesis [9–18]. This protein is redistributed from the nucleus to the cytoplasm and forms aggregates in affected neurons and glial cells of SALS patients [1–3] (Fig. 2), suggesting that gain and/or loss of TDP-43 function underlies SALS pathogenesis. With regard to gain of TDP-43 toxicity, rodent and primate models overexpressing wild-type or disease-mutant TDP-43 exhibit the phenotype of neurodegeneration, but this exogenous TDP-43 exists mainly in the nuclei, and TDP-43-positive cytoplasmic inclusions are barely detectable [19–28]. Although it is unclear how wild-type and mutant TDP-43 acquire a toxic effect, overexpression of TDP-43 makes a dose-dependent contribution to neurodegeneration [20–22]. In addition, pathological *TARDBP* mutations have longer half-lives compared to the wild type [29, 30], and longer half-lives of mutant proteins are correlated with accelerated disease onset [30], suggesting that mutant TDP-43 toxicity depends on its protein stability. On the other hand, *TARDBP* knockout mice are embryonic lethal [31–33], and postnatal deletion of *TARDBP* led to rapid loss of body fat and death [34]. Finally, motor neuron-specific *TARDBP* knockout mice exhibited age-dependent progressive motor dysfunction together with ALS-mimicking pathology, including motor axonal degeneration, neurogenic muscle atrophy, and denervation at neuromuscular junctions [35, 36] (Fig. 3). These lines of evidence suggest that both gain and loss of TDP-43 function contribute to ALS pathogenesis.

FUS

Mutations in the gene encoding fused in sarcoma (FUS) mutations have been identified in autosomal dominant FALS, which accounts for ~4 % of FALS cases [37–39]. The majority of *FUS* mutations are in the C-terminal nuclear localization signal (NLS), and these mutants cause aberrant cytoplasmic distributions of FUS [37, 38]. Although the majority of patients carrying *FUS* mutations exhibit a classical ALS phenotype without cognitive impairment, the clinical courses of these ALS patients are diverse, even among carriers of the same mutations [40–44]. The FUS protein has been demonstrated in neuronal cytoplasmic inclusions in ALS cases with *FUS* mutations and a subset of FTLD with ubiquitinated, neuronal intermediate filament inclusion disease (NINID), and basophilic

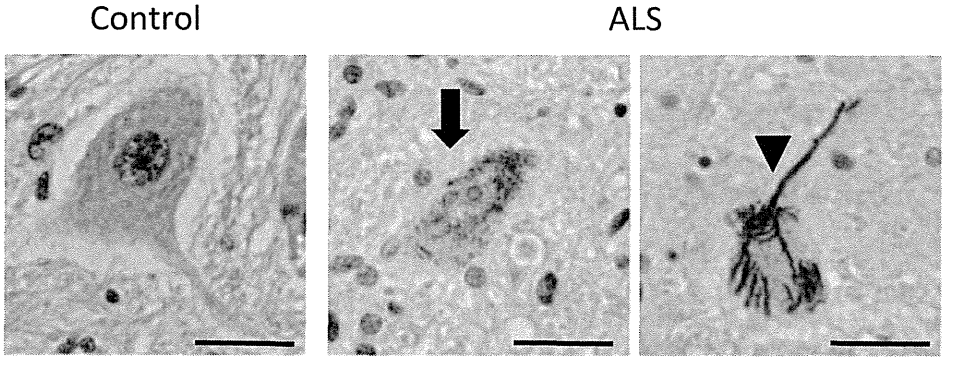

Fig. 2 TDP-43 pathology of spinal motor neuron. Lumbar spinal cords of control and ALS patients were stained with anti-TDP-43 antibody (Proteintech). TDP-43 is normally localized in the nucleus, but is redistributed to the cytoplasm in various patterns, such as a diffuse granular distribution (*arrow*) and skein-like inclusions (*arrow head*). The *scale bars* represent 20 μm

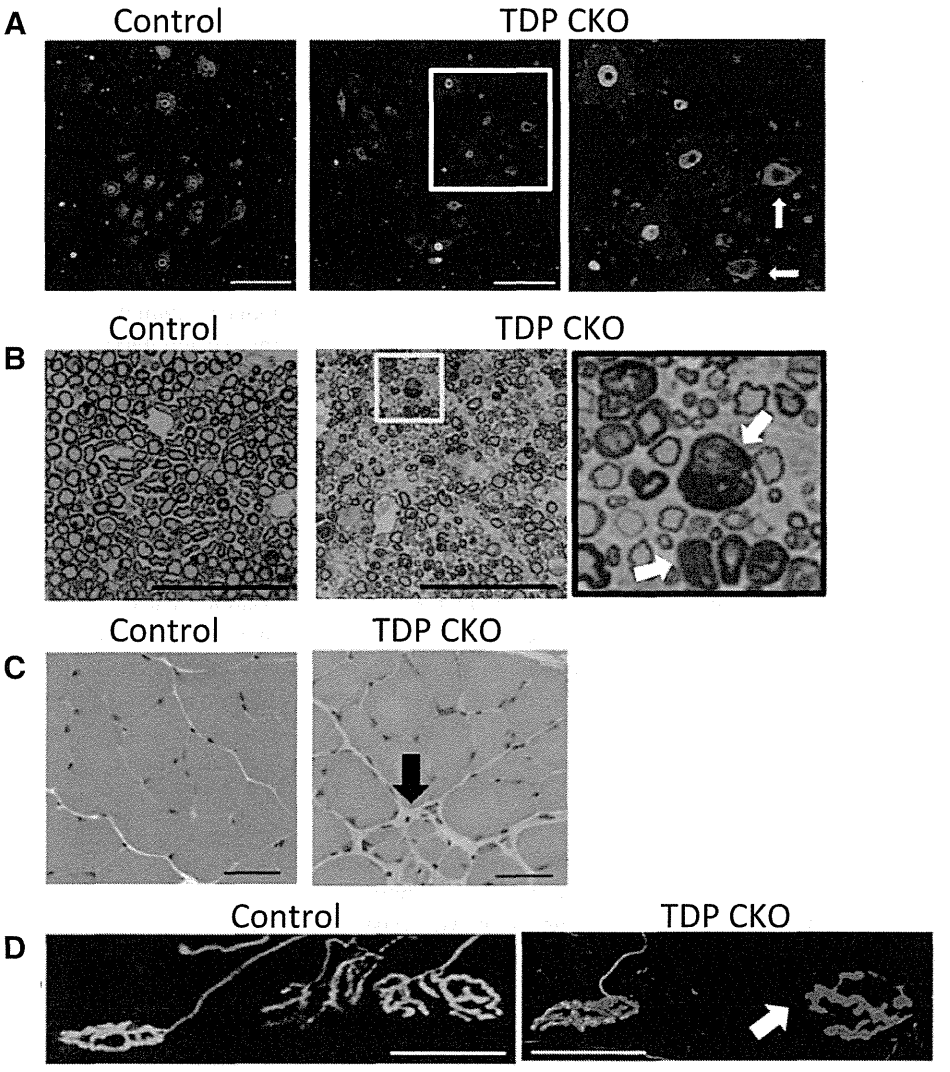

Fig. 3 Motor neuron-specific TDP-43 knockout (TDP CKO) mice exhibit degeneration of the motor neuron system. **a** Immunofluorescencent stainings (TDP-43, *green*; ChAT, *red*) of the lumbar ventral horn from 100-week-old control and TDP CKO mice. TDP-43-lacking motor neurons (*arrows*) were significantly smaller than TDP-43-positive motor neurons. **b** Toluidine blue-stained images in the L5 ventral root from 100-week-old control and TDP CKO mice. *Arrows* indicate axonal degeneration. The *scale bars* represent 100 μm. **c** Hematoxylin and eosin staining of gastrocnemius muscles of 100-week-old mice. Axial sections from TDP CKO mice exhibited grouped atrophy (*arrow*). **d** Immunofluorescent staining (synaptophysin and phopsho-neurofilament, *green*; bungarotoxin, *red*) of NMJs in 100-week-old mice. Denervated NMJs (*arrow*) are indicated by the lack of staining of synaptophysin and phospho-neurofilament. The *scale bar* represents 50 μm. Reproduced with permission from Iguchi et al. Ref. [36]

inclusion body disease (BIBD) [45–48]. These inclusions are positive for GRP78/BiP, p62 and ubiquitin, but not for TDP-43 [38, 49, 50]. In addition, FUS is reported to be co-localized with ubiquitin and TDP-43-positive cytoplasmic inclusions of SALS patients [51, 52]. This issue remains controversial, however, because in other studies, FUS was not found in these inclusions in SALS [38, 47, 53]. Rat models overexpressing human disease mutants of *FUS* exhibit pathological phenotypes like ALS and FTLD [54], and overexpression of human wild-type FUS in mice causes dose-dependent progressive motor neuron degeneration [55]. By contrast, *FUS* knockout mice on an inbred C57BL/6 background display perinatal death and exhibit abnormal lymphocytes and chromosomal instability [56], whereas knockout mice on an outbred background develop male sterility and survive until adulthood [57]. It is noteworthy that FUS and TDP-43 share structural and functional similarities [58] and that both proteins regulate alternative pre-mRNA splicing events and transcription [59–62]. Although most of the mRNA targets for FUS are distinct from those for TDP-43, a small set of common targets may contribute to ALS pathogenesis [60, 61]. In addition, both TDP-43 and FUS associate with the SMN complex and are involved in spliceosome maintenance [63, 64].

FIG4

FIG4 was reported as a causative gene for Charcot-Marie-Tooth disease type 4J (CMT4J), an autosomal recessive motor and sensory neuropathy [65]. Later, *FIG4* mutations were identified in autosomal-dominant FALS and SALS [66]. In this cohort of European ancestry, *FIG4* mutations were found in 2 % of ALS and primary lateral sclerosis (PLS) cases [66]. Two of ten identified mutations are truncation mutations that lead to loss of FIG4 phosphatase

activity [66]. The protein transcript of *FIG4* is a phosphoinositide 5-phosphatase that regulates a cellular abundance of phosphatidylinositol 3,5-bisphosphate (PI(3,5)P2), a signaling lipid on the cytosolic surface of membranes of the late endosomal compartment [67]. PI(3,5)P2 is required for retrograde membrane trafficking from lysosomal and late endosomal compartments to the Golgi and is involved in autophagy [68–70]. The analysis of *FIG4*$^{-/-}$ mouse brain shows disruption of autophagy in neurons and glial cells [71].

OPTN

Three mutations of *OPTN* were identified in Japanese FALS patients [72], with both dominant and recessive mutations observed. Later analyses in Japanese and European populations revealed several additional mutations, and estimated mutation rates were 1–4 % in FALS [73–75]. Although optineurin, which is encoded by *OPTN,* regulates TNFα-induced NF-κB activation negatively by binding to polyubiquitinated RIP [76], ALS-causative *OPTN* mutations abolish its inhibition [72]. OPTN also acts as an autophagy receptor [77] and coordinates actin-based and microtubule-based motor function for maintenance of Golgi morphology [78]. OPTN is co-localized in ubiquitinated neuronal cytoplasmic inclusions of SALS spinal cords [72, 79–81], suggesting that OPTN is generally involved in the pathogenesis of a variety of ALS types.

ATXN2

The pathological expansions (>34 repeats) of a CAG repeat in *ATXN2,* which encodes a polyglutamine tract in ataxin-2, cause spinocerebellar ataxia type 2 (SCA2). Intermediate-length expansions (27–33 glutamine residues) were reported to contribute to susceptibility to ALS [82]. In a later study, however, longer *ATXN2* repeats (>29–32 repeats) were significantly associated with the disease [83–86], and CAG repeats (≥32) were found in approximately 2 % of familial and sporadic ALS patients [84]. Furthermore, Expanded *ATXN2* repeats were also significantly associated with progressive supranuclear palsy [87]. Pathological analysis shows that ataxin-2 forms cytoplasmic aggregates in ALS spinal cord neurons, although this protein is localized in a diffuse or fine-granular pattern throughout the cytoplasm of control spinal cord neurons [82]. Although the pathological mechanism of *ATXN2* expansion in ALS pathogenesis is not fully understood, CAG repeat expansions are reported to enhance the interaction between ataxin-2 and TDP-43 or mutant FUS [82, 88].

DAO

D-serine, a co-agonist of the *N*-methyl D-aspartate (NMDA) type of glutamate receptor [89], was reported to accumulate in the spinal cords of SALS and G93A SOD1 mice [90, 91]. D-amino acid oxidase (DAO) negatively regulates D-serine. Mutation R199W in the *DAO* gene was identified in autosomal dominant FALS [92]. This mutation, when expressed in neuronal cell lines, reduces cell viabilities and induces ubiquitinated aggregates [92]. These data suggest that accumulation of D-serine contributes to an ALS pathogenesis, and DAO might be a common therapeutic target for ALS.

SPG11

Mutations of the spatacsin gene (*SPG11*) are the most common cause of hereditary spastic paraplegia with thinning corpus callosum [93]. Recently, *SPG11* mutations were identified in autosomal recessive juvenile ALS [94]. These patients exhibit a slowly progressive phenotype of motor neuron disease. Although the loss-of-function mechanism is suggested as the pathogenesis of ALS with the *SPG11* mutation, the physiological function of this molecule is unclear.

VCP

Mutations in *VCP* were found in patients with inclusion body myopathy of early-onset Paget disease and frontotemporal dementia (IBMPFD) [95]. In addition, *VCP* mutation was identified in 1–2 % of FALS cases with or without the phenotype of IBMPFD in an autosomal dominant manner [96]. Now, IBMPFD is referred to as a multisystem proteinopathy (MSP), which affects motor neurons, brain, skeletal muscle, and bone. *VCP* mutation carriers exhibit diverse phenotypes, even with the same mutation [97]. TDP-43 positive ubiquitinated cytoplasmic inclusions in the affected neurons are present in patients with *VCP* mutations [96, 98]. The highly conserved AAA+-ATPase, VCP regulates multiple cellular pathways such as the ubiquitin–proteasome system (UPS), autophagy, endosomal sorting, and regulating protein degradation at the outer mitochondrial membrane, and chromatin-associated processes [99]. VCP is indispensable for maturation of autophagosomes, and disease-causative mutations of VCP disrupt this process [100]. Mutant VCP knock-in mice develop age-dependent motor dysfunction with abnormal TDP-43 pathologies in the spinal cord, muscle and brain [101–103].

UBQLN2

Mutations in *UBQLN2* were identified in rare X-linked dominant ALS cases [104]. UBQLN2-positive inclusions are found in the spinal cord of ALS and ALS/FTLD patients with *UBQLN2* mutations, and these inclusions frequently contain TDP-43 and FUS [104, 105]. In addition, abnormal UBQLN2 pathologies are found in SALS patients and FUS mutation carriers [104, 105]. These data suggest that UBQLN2 is generally involved in the pathogenesis of ALS. UBQLN2 is a member of the ubiquilin family, which is involved in both the ubiquitin–proteasome system and autophagy [106, 107], and mutations in *UBQLN2* were reported to disrupt protein degradation [104].

C9ORF72

In a large family with FTLD and/or ALS mapping to chromosome 9p21, a GGGGCC hexanucleotide repeat was identified between noncoding exons 1a and 1b of the *C9ORF72* gene [108, 109]. The repeat is <25 units in healthy controls, whereas the estimated expansion range is from 800 to 4,400 units in cases carrying this repeat expansion [108–110]. The mutation frequencies in European and North American Caucasian populations are generally high: they are up to 29, 50 and 88 % in FTLD, ALS and ALS/FTLD patients [111]. Especially in North Europe, the repeat expansion frequencies are from 12 to 21 %, even in the SALS patients [108, 112, 113]. By contrast, the frequency of ALS patients with these expansions is very low in Asian populations [113–119]. ALS patients with C9ORF72 expansion commonly have a bulbar onset and cognitive impairment and partially exhibit Parkinsonism or psychiatric symptoms such as psychosis or suicide [120–122]. Abundant UBQLN-positive cytoplasmic inclusions are seen in the cerebellum and the hippocampus. UBQLN is co-localized partially with p62 and only rarely with TDP-43 positive inclusions [123, 124]. Using RNA fluorescence in situ hybridization (FISH) analysis, C9ORF72-containing RNA foci are observed in 25 % of the spinal cord and frontal cortical neurons of patients with the repeat expansion [108]. In addition, the neurons contain dipeptide repeat proteins generated from this intronic repeat region by non-ATG-initiated translation [125, 126]. It is, however, uncertain whether these neuronal accumulations of the aberrant RNA, and protein derived from C9ORF72 repeat expansions contribute to the neurodegeneration. The latest study demonstrated that C9ORF72 is a full-length distant homologue of proteins related to DENN, which is a Rab GEF, a regulator of Rab-GTPase activity [127]. Because Rab GTPases regulate membrane trafficking, C9ORF72 may have a crucial role in neuronal activities such as axonal transport and the autophagy-lysosome system. Although no reliable antibody for this protein is known, the intronic repeat expansions are reported to cause the loss of one or all alternatively spliced C9ORF72 transcripts [108, 109, 128], suggesting that C9ORF72 haploinsufficiency may underlie the pathogenesis of ALS patients carrying this repeat expansion. The high incidence of C9ORF72 mutations in Caucasian ALS patients raises the possibility of the additional identification for ALS-causative gene mutations, even in SALS. Targeting a specific molecule, such as C9ORF72, appears to be a promising strategy.

PFN1

PFN1 mutations were identified in autosomal dominant FALS patients, [129]. Although four missense mutations were reported in 274 FALS patients [129], several other analyses further suggest that the mutation carriers in FALS patients are generally rare [130–138]. Profilin-1, the protein transcript of *PFN1,* is essential for the polymerization of monomeric G-actin to form filamentous actin [139]. A disrupted mutant of *PFN1* causes a growth cone arrest in embryonic motor neurons of Drosophila [140]. Although the neuropathology of an ALS patient with the *PFN1* mutation is not reported, ALS-related mutants of *PFN1* form ubiquitinated cytoplasmic aggregates when they are overexpressed in Neuro-2a cells or primary motor neurons [129]. In addition, the *PFN1* mutants reduce actin-binding ability, inhibit axonal outgrowth, and reduce the size of the growth cone in cultured cells or primary motor neurons [129]. These findings suggest that mutation-dependent disruption of *PFN1* function contributes to ALS pathogenesis via an alteration of the actin dynamic pathway.

SIGMAR1

SIGMAR1 is reported to be associated with juvenile amyotrophic sclerosis. A homozygous missense mutation, E102Q, in *SIGMAR1* gene was identified in autosomal recessive FALS from Saudi Arabia [141]. Patients carrying the *SIGMAR1* mutation exhibit the motor neuron disease phenotype at the age of 1–2 years, and the weakness progresses slowly without cognitive impairment. The sigma-1 receptor (S1R), which is encoded by *SIGMAR1*, is a non-steroidal ER protein that regulates various ion channel activities and has a protein chaperone function [142]. S1R is highly expressed in motor neurons of the brain stem and spinal cord, and S1R knockout mice are reported to have motor deficiency [143]. These findings suggest that the mutation in *SIGMAR1* affects predominantly motor neurons via loss of S1R function. Further investigations,

including a histopathological characterization of post-mortem samples and functional analysis of the S1R mutant, are needed.

Molecular targeted approach for the treatment of ALS

Current therapies for neurodegenerative diseases are targeted mainly to symptomatic relief or replacement of neurotransmitters. Most of these therapies, however, do not halt or reduce neurodegenerative progression [144]. With regard to ALS, the only available drug, riluzole (6-(trifluoromethoxy)benzothiazol-2-amine), has a limited effect: the increase in median survival for the riluzole-treated group was 2–3 months [145]. Many compounds, including vitamin E, gabapentin, topiramate, creatine, celecoxib and minocycline, identified in studies using animal models have failed in the clinical trials of ALS.

Although several interpretations can be considered, one possibility of the cause of this divergence is the use of mutant SOD1 mice in pre-clinical studies. There are distinct pathophysiological differences between SOD1-mediated FALS (ALS1) and SALS [146, 147]. Conversely, TDP-43 is a promising therapeutic target for SALS, because abnormal TDP-43 pathologies are characteristic features of SALS. Given that a dose-dependent or aggregate toxicity of TDP-43 would be related to ALS pathogenesis, interventions to regulate TDP-43 protein expression or to mitigate the aggregate formation could have therapeutic potential for ALS. An analysis using induced pluripotent stem (iPS) cells derived from ALS patients carrying TDP-43 mutations would be a useful tool for elucidating ALS disease pathogenesis and for screening drug candidates [148].

Analyzing functional similarities to ALS-causative molecules is a promising approach. Some of these molecules share physiological functions indispensable for cellular activities, including RNA metabolism, protein degradation, and the ER-Golgi pathway (Fig. 1). For instance, several ALS-causative genes, including *VCP, UBQLN2, OPTN* and *FIG4,* are related to a protein-degrading system via autophagy, and mutations in *SQSTM1*, which encodes p62, have been identified in ALS patients [149]. ALS patients carrying mutations in these genes have TDP-43-positive neuronal cytoplasmic inclusions, suggesting that the effect of these mutations could be an upstream cause for the aberrant TDP-43 pathology. In addition, p62-positive neuronal inclusions are seen in most of SALS and FALS patients, and accumulations of autophagosomes are observed in the motor neurons of SALS patients [150]. These lines of data suggest that dysregulation of autophagy commonly underlies ALS pathogenesis. Notably, autophagy activators rescue the phenotype and pathology in FTLD model mice in which wild-type TDP-43 was overexpressed in the forebrain [151], suggesting that the autophagic pathway could be a potential therapeutic target for ALS.

TDP-43, FUS, and ataxin-2 are components of stress granules (SGs), which have a central role in the stress response, such as regulating mRNA translation and turnover [152] under stress [153–155]. In addition, the TDP-43 C-terminal fragment and FUS-disease mutant are recruited more abundantly into SGs [156–158]. Given that stress granule marker proteins are co-localized in TDP-43 and FUS-positive neuronal inclusions of ALS and FTLD patients [158, 159], dysregulation of mRNA metabolism in SGs would underlie common ALS pathogenesis and could be a therapeutic target for ALS. Furthermore, TDP-43 and FUS have a similar sequence to the prion protein, prion-like domain (PrLD). Notably, an insoluble fraction of TDP-43 from FTLD brain has a seeding ability when introduced into cultured cells, and the aggregated TDP-43 induced by these seeds is propagated to neighboring cells [160]. These data suggest that interference with the propagation of TDP-43 or other RNA-binding proteins may be a therapeutic target for ALS. Finally, mutations in other RNA-binding proteins, such as Ewing's sarcoma breakpoint region 1 (EWSR1), TATA-binding protein-associated factor 15 (TAF15), and heterogeneous nuclear ribonucleoprotein A1 (hnRNPA1) have been identified in ALS patients [161–163]. These RNA-binding proteins are responsible for RNA metabolism and harbor a PrLD as well as TDP-43 and FUS.

ALS causative genes have been uncovered by recent developments in gene analysis technology. Certain FALS-causing gene mutations have also been identified in SALS cases, suggesting that sporadic and familial forms of ALS share, at least in part, the same molecular pathomechanism. These discoveries provide novel insight into ALS pathogenesis and are expected to contribute to developing an effective disease-modifying therapy. Given the limited availability of animal models carrying FALS mutations, the results of genetic studies should be utilized for the creation of models and the search for therapies that suppress motor neuron degeneration.

Acknowledgments This work was supported by Grant-in-Aids (KAKENHI) from the Ministry of Education, Culture, Sports, Science, and Technology of Japan (Nos. 22110005, 21229011 and 23390230) and Core Research for Evolutional Science and Technology (CREST) from the Japan Science and Technology Agency (JST). Figure 3 was reproduced from Iguchi et al. Ref. [36].

Conflicts of interest None.

References

1. Arai T, Hasegawa M, Akiyama H et al (2006) TDP-43 is a component of ubiquitin-positive tau-negative inclusions in

frontotemporal lobar degeneration and amyotrophic lateral sclerosis. Biochem Biophys Res Commun 351:602–611
2. Neumann M, Sampathu DM, Kwong LK et al (2006) Ubiquitinated TDP-43 in frontotemporal lobar degeneration and amyotrophic lateral sclerosis. Science 314:130–133
3. Mackenzie IR, Neumann M, Cairns NJ et al (2011) Novel types of frontotemporal lobar degeneration: beyond tau and TDP-43. J Mol Neurosci 45:402–408
4. Gitcho MA, Baloh RH, Chakraverty S et al (2008) TDP-43 A315T mutation in familial motor neuron disease. Ann Neurol 63:535–538
5. Kabashi E, Valdmanis PN, Dion P et al (2008) TARDBP mutations in individuals with sporadic and familial amyotrophic lateral sclerosis. Nat Genet 40:572–574
6. Sreedharan J, Blair IP, Tripathi VB et al (2008) TDP-43 mutations in familial and sporadic amyotrophic lateral sclerosis. Science 319:1668–1672
7. Yokoseki A, Shiga A, Tan CF et al (2008) TDP-43 mutation in familial amyotrophic lateral sclerosis. Ann Neurol 63:538–542
8. Corcia P, Valdmanis P, Millecamps S et al (2012) Phenotype and genotype analysis in amyotrophic lateral sclerosis with TARDBP gene mutations. Neurology 78:1519–1526
9. Wang HY, Wang IF, Bose J et al (2004) Structural diversity and functional implications of the eukaryotic TDP gene family. Genomics 83:130–139
10. Ayala YM, Pantano S, D'Ambrogio A et al (2005) Human, Drosophila, and C. elegans TDP43: nucleic acid binding properties and splicing regulatory function. J Mol Biol 348:575–588
11. Buratti E, Brindisi A, Giombi M et al (2005) TDP-43 binds heterogeneous nuclear ribonucleoprotein A/B through its C-terminal tail: an important region for the inhibition of cystic fibrosis transmembrane conductance regulator exon 9 splicing. J Biol Chem 280:37572–37584
12. Strong MJ, Volkening K, Hammond R et al (2007) TDP43 is a human low molecular weight neurofilament (hNFL) mRNA-binding protein. Mol Cell Neurosci 35:320–327
13. Buratti E, De Conti L, Stuani C et al (2010) Nuclear factor TDP-43 can affect selected microRNA levels. FEBS J 277:2268–2281
14. Polymenidou M, Lagier-Tourenne C, Hutt KR et al (2011) Long pre-mRNA depletion and RNA missplicing contribute to neuronal vulnerability from loss of TDP-43. Nat Neurosci 14:459–468
15. Tollervey JR, Curk T, Rogelj B et al (2011) Characterizing the RNA targets and position-dependent splicing regulation by TDP-43. Nat Neurosci 14:452–458
16. Sephton CF, Cenik C, Kucukural A et al (2011) Identification of neuronal RNA targets of TDP-43-containing ribonucleoprotein complexes. J Biol Chem 286:1204–1215
17. Xiao S, Sanelli T, Dib S et al (2011) RNA targets of TDP-43 identified by UV-CLIP are deregulated in ALS. Mol Cell Neurosci 47:167–180
18. Kawahara Y, Mieda-Sato A (2012) TDP-43 promotes microRNA biogenesis as a component of the Drosha and Dicer complexes. Proc Natl Acad Sci USA 109:3347–3352
19. Wegorzewska I, Bell S, Cairns NJ et al (2009) TDP-43 mutant transgenic mice develop features of ALS and frontotemporal lobar degeneration. Proc Natl Acad Sci USA 106:18809–18814
20. Wils H, Kleinberger G, Janssens J et al (2010) TDP-43 transgenic mice develop spastic paralysis and neuronal inclusions characteristic of ALS and frontotemporal lobar degeneration. Proc Natl Acad Sci USA 107:3858–3863
21. Xu YF, Gendron TF, Zhang YJ et al (2010) Wild-type human TDP-43 expression causes TDP-43 phosphorylation, mitochondrial aggregation, motor deficits, and early mortality in transgenic mice. J Neurosci 30:10851–10859
22. Stallings NR, Puttaparthi K, Luther CM et al (2010) Progressive motor weakness in transgenic mice expressing human TDP-43. Neurobiol Dis 40:404–414
23. Zhou H, Huang C, Chen H et al (2010) Transgenic rat model of neurodegeneration caused by mutation in the TDP gene. PLoS Genet 6:e1000887
24. Tsai KJ, Yang CH, Fang YH et al (2010) Elevated expression of TDP-43 in the forebrain of mice is sufficient to cause neurological and pathological phenotypes mimicking FTLD-U. J Exp Med 207:1661–1673
25. Shan X, Chiang PM, Price DL et al (2010) Altered distributions of Gemini of coiled bodies and mitochondria in motor neurons of TDP-43 transgenic mice. Proc Natl Acad Sci USA 107:16325–16330
26. Swarup V, Phaneuf D, Bareil C et al (2011) Pathological hallmarks of amyotrophic lateral sclerosis/frontotemporal lobar degeneration in transgenic mice produced with TDP-43 genomic fragments. Brain 134:2610–2626
27. Arnold ES, Ling SC, Huelga SC et al (2013) ALS-linked TDP-43 mutations produce aberrant RNA splicing and adult-onset motor neuron disease without aggregation or loss of nuclear TDP-43. Proc Natl Acad Sci USA 110:E736–E745
28. Uchida A, Sasaguri H, Kimura N et al (2012) Non-human primate model of amyotrophic lateral sclerosis with cytoplasmic mislocalization of TDP-43. Brain 135:833–846
29. Ling SC, Albuquerque CP, Han JS et al (2010) ALS-associated mutations in TDP-43 increase its stability and promote TDP-43 complexes with FUS/TLS. Proc Natl Acad Sci USA 107:13318–13323
30. Watanabe S, Kaneko K, Yamanaka K (2013) Accelerated disease onset with stabilized familial amyotrophic lateral sclerosis (ALS)-linked mutant TDP-43 proteins. J Biol Chem 288: 3641–3654
31. Wu LS, Cheng WC, Hou SC et al (2010) TDP-43, a neuropathosignature factor, is essential for early mouse embryogenesis. Genesis 48:56–62
32. Sephton CF, Good SK, Atkin S et al (2010) TDP-43 is a developmentally regulated protein essential for early embryonic development. J Biol Chem 285:6826–6834
33. Kraemer BC, Schuck T, Wheeler JM et al (2010) Loss of murine TDP-43 disrupts motor function and plays an essential role in embryogenesis. Acta Neuropathol 119:409–419
34. Chiang PM, Ling J, Jeong YH et al (2010) Deletion of TDP-43 down-regulates Tbc1d1, a gene linked to obesity, and alters body fat metabolism. Proc Natl Acad Sci USA 107:16320–16324
35. Wu LS, Cheng WC, Shen CK (2012) Targeted depletion of TDP-43 expression in the spinal cord motor neurons leads to the development of amyotrophic lateral sclerosis-like phenotypes in mice. J Biol Chem 287:27335–27344
36. Iguchi Y, Katsuno M, Niwa J et al (2013) Loss of TDP-43 causes age-dependent progressive motor neuron degeneration. Brain 136:1371–1382
37. Kwiatkowski TJ Jr, Bosco DA, Leclerc AL et al (2009) Mutations in the FUS/TLS gene on chromosome 16 cause familial amyotrophic lateral sclerosis. Science 323:1205–1208
38. Vance C, Rogelj B, Hortobagyi T et al (2009) Mutations in FUS, an RNA processing protein, cause familial amyotrophic lateral sclerosis type 6. Science 323:1208–1211
39. Van Langenhove T, van der Zee J, Sleegers K et al (2010) Genetic contribution of FUS to frontotemporal lobar degeneration. Neurology 74:366–371
40. Yan J, Deng HX, Siddique N et al (2010) Frameshift and novel mutations in FUS in familial amyotrophic lateral sclerosis and ALS/dementia. Neurology 75:807–814